p63 is an alternative p53 repressor in melanoma that confers chemoresistance and a poor prognosis

Rubeta N. Matin,[1] Anissa Chikh,[1] Stephanie Law Pak Chong,[1] David Mesher,[2] Manuela Graf,[1] Paolo Sanza',[1] Valentina Senatore,[1] Maria Scatolini,[4] Francesca Moretti,[5] Irene M. Leigh,[6] Charlotte M. Proby,[6] Antonio Costanzo,[5] Giovanna Chiorino,[4] Rino Cerio,[3] Catherine A. Harwood,[1] and Daniele Bergamaschi[1]

[1]Centre for Cutaneous Research, Blizard Institute; [2]Centre for Cancer Prevention, Wolfson Institute of Preventive Medicine; and [3]Pathology Group; Barts and The London School of Medicine and Dentistry, Queen Mary University of London, London E1 2AT, England, UK
[4]Cancer Genomic Laboratory, Edo ed Elvo Tempia Foundation, 13900 Biella, Italy
[5]Dermatology Unit, Neurosciences, Mental Health, and Sensory Functions (NESMOS) Department, School of Medicine and Psychology, Sapienza University of Rome, 00189 Rome, Italy
[6]Division of Cancer Research, Medical Research Institute, College of Medicine, Dentistry, and Nursing, Ninewells Hospital, University of Dundee, Dundee DD1 9SY, Scotland, UK

The role of apoptosis in melanoma pathogenesis and chemoresistance is poorly characterized. Mutations in TP53 occur infrequently, yet the TP53 apoptotic pathway is often abrogated. This may result from alterations in TP53 family members, including the TP53 homologue TP63. Here we demonstrate that TP63 has an antiapoptotic role in melanoma and is responsible for mediating chemoresistance. Although p63 was not expressed in primary melanocytes, up-regulation of p63 mRNA and protein was observed in melanoma cell lines and clinical samples, providing the first evidence of significant p63 expression in this lineage. Upon genotoxic stress, endogenous p63 isoforms were stabilized in both nuclear and mitochondrial subcellular compartments. Our data provide evidence of a physiological interaction between p63 with p53 whereby translocation of p63 to the mitochondria occurred through a codependent process with p53, whereas accumulation of p53 in the nucleus was prevented by p63. Using RNA interference technology, both isoforms of p63 (TA and ΔNp63) were demonstrated to confer chemoresistance, revealing a novel oncogenic role for p63 in melanoma cells. Furthermore, expression of p63 in both primary and metastatic melanoma clinical samples significantly correlated with melanoma-specific deaths in these patients. Ultimately, these observations provide a possible explanation for abrogation of the p53-mediated apoptotic pathway in melanoma, implicating novel approaches aimed at sensitizing melanoma to therapeutic agents.

CORRESPONDENCE
Daniele Bergamaschi:
d.bergamaschi@qmul.ac.uk

Abbreviations used: HR, hazard ratio; mTMA, melanoma tissue microarray; PI, propidium iodide; PIC, protease inhibitor cocktail; Q-PCR, quantitative PCR; RGP, radial growth phase; RNAi, RNA interference.

Apoptotic dysregulation is a hallmark of melanoma pathogenesis and chemoresistance. Mutations in *TP53* occur infrequently in melanoma (Weiss et al., 1995; Zerp et al., 1999; Hocker and Tsao, 2007; Ji et al., 2012) and are not critical for tumor development (Stretch et al., 1991; Lassam et al., 1993; Kanoko et al., 1996; Zerp et al., 1999). Nevertheless, the TP53 apoptotic pathway is abrogated in melanoma; this may result from dysregulation of upstream (Matsuoka et al., 1998; Chehab et al., 2000; Hirao et al., 2000; Shieh et al., 2000) or downstream TP53 cell signaling (Bae et al., 1996; Satyamoorthy et al., 2000) or from alterations in other members of the TP53 family (Tuve et al., 2006), including the *TP53* homologue *TP63*. To date, there is limited evidence to explain the mechanism or mechanisms of inactivation or attenuation of p53 tumor suppression in melanomagenesis. Whole genome array studies have demonstrated

R.N. Matin and A. Chikh contributed equally to this paper.

The Rockefeller University Press $30.00
J. Exp. Med. 2013 Vol. 210 No. 3 581-603
www.jem.org/cgi/doi/10.1084/jem.20121439

a failure of p53 to regulate target genes involved in cell cycle and apoptosis (Hoek et al., 2004; Prince et al., 2004; Karst et al., 2005; Vance et al., 2005; Avery-Kiejda et al., 2011), raising the possibility that aberrant functioning of the p53 pathway promotes melanoma progression (Avery-Kiejda et al., 2011).

High levels of p53 expression in melanoma cells and tissue samples have been reported in numerous studies (Bártek et al., 1991; Stretch et al., 1991; Akslen and Mørkve, 1992; McGregor et al., 1993; Yamamoto et al., 1995; Hussein et al., 2003; Houben et al., 2011; Knopf et al., 2011). This is often in the absence of point mutations in the gene (McGregor et al., 1993; Albino et al., 1994; Sparrow et al., 1995) but is associated with transcriptional inactivity (Houben et al., 2011). Moreover, correlation of p53 immunoreactivity with advanced melanoma and unfavorable prognosis has been demonstrated (McGregor et al., 1993; Yamamoto et al., 1995). Small molecular weight variants of p53 have also been demonstrated in melanoma and, in some instances, are expressed at higher levels than full-length WT-p53 (Avery-Kiejda et al., 2008).

This study focuses on *TP63*, a gene which is tissue-specifically transcribed into *TA* and *ΔN* isoforms by two alternative promoters (Osada et al., 1998; Yang et al., 1998). Both *TA* and *ΔN* isoforms undergo three alternative splicing events at the C terminus, generating six different isoforms (Ikawa et al., 1999; Yang and McKeon, 2000; Mills, 2006). More recently, two new C-terminal *TP63* variants, named *TP63* δ and ε, have also been identified, bringing the total number of *TP63* isoforms to 10 (Mangiulli et al., 2009). To date, the p63 proteins display a diverse range of biological activities, impacting cells in an isoform-dependent but also cell type– and stimulus-specific manner. p63 plays a complex role in tumorigenesis that is likely to be context specific (Flores et al., 2005; Keyes et al., 2005; Perez-Losada et al., 2005); p63 genomic locus amplification and/or overexpression of ΔNp63 occurs in 80% of head and neck squamous cell carcinomas, supporting its role as an oncogene (Hibi et al., 2000; Yang and McKeon, 2000; Choi et al., 2002; Hu et al., 2002; Massion et al., 2003; Mills, 2006).

The expression pattern of p63 isoforms has not been widely investigated in melanoma. Previous studies of p63 in melanocytes are conflicting; mouse melanocytes express two isoforms of p63, *TAp63β* and either *TAp63γ* or *ΔNp63β* (Kulesz-Martin et al., 2005), and cultured human eye melanocytes do not express *TP63* (Kilic et al., 2008). Neither of these studies were adequate biological correlates for human cutaneous melanocytes: mouse melanocytes predominantly reside in the hair follicle within the dermis, mice do not spontaneously develop melanoma (Bardeesy et al., 2000; Merlino and Noonan, 2003), and the molecular biology of ocular melanoma is distinct from cutaneous melanoma (Belmar-Lopez et al., 2008; Sato et al., 2008; Shields et al., 2008). Studies using immunohistochemistry techniques to investigate expression of p63 protein in human melanoma have mostly used it as an example of negative reactivity; in two tissue microarrays, *ΔNp63* was expressed in 2/59 (3.4%) and 2/25 (8%) human melanomas (Reis-Filho et al., 2003a). A more recent study demonstrated expression in 1/20 (5%) desmoplastic melanomas (Kanner et al., 2010). Expression of *TAp63* and *ΔNp63* in uveal melanoma was demonstrated in 12/18 (66.7%) and 1/18 (5.6%) cell lines, respectively (Kilic et al., 2008). Other studies have suggested a lack of p63 expression in melanoma in situ or invasive disease (Di Como et al., 2002; Dotto and Glusac, 2006; Bourne et al., 2008; Morgan et al., 2008; Sakiz et al., 2009; Glusac, 2011).

The tissue-specific response of p63 to DNA damage is variable. The only study investigating p63 response in the melanocyte lineage reported expression of two isoforms: TAp63β and either TAp63γ or ΔNp63β (undetermined) in mouse melanocytes with no endogenous up-regulation in mouse melanoma cells. In this mouse model, p63 isoforms were not induced upon DNA damage (Kulesz-Martin et al., 2005). In contrast, ectopically expressed TAp63α and γ isoforms accumulate in leukemic cells in response to UVB, UVC, doxorubicin, and etoposide (Katoh et al., 2000; Okada et al., 2002). To support this, topoisomerase II inhibitors (doxorubicin and etoposide) but not UVB induced endogenous expression of TAp63α (and p53-target genes *p21*, *14-3-3-σ*, *GADD45*, and *PIG3*) but not *ΔNp63* in mouse hepatocytes and human hepatocellular carcinoma cells (Petitjean et al., 2005). A consistent picture emerges whereby certain forms of DNA damage induce an apoptotic response mediated, at least in part, through degradation of antiapoptotic ΔN isoforms (Liefer et al., 2000; Harmes et al., 2003) and stabilization of proapoptotic TA isoforms (Gressner et al., 2005).

There is intense debate as to whether, and how, p53 family members interact with each other in apoptosis and tumor suppression (Benchimol, 2004). Induction of death by p53 requires partnership of p63 and p73 in neurons and mouse embryo fibroblasts (Flores et al., 2002). This effect may be tissue specific as p63 and p73 are not required for the induction of apoptosis in T cells (Senoo et al., 2004). In neuronal cells, although p63 alone can promote neuronal apoptosis, it is also an obligate proapoptotic partner for p53 and essential for p53-induced apoptotic cell death (Jacobs et al., 2005). In hepatocellular carcinoma, all three p53 family members were involved in the DNA damage response to genotoxic agents, revealing a central role for the p53/p63/p73 network in treatment response and prognosis of this cancer (Gressner et al., 2005; Müller et al., 2006; Mundt et al., 2010; Schilling et al., 2010; Seitz et al., 2010).

p53 is best characterized as a nuclear transcription factor that transactivates various genes (Riley et al., 2008). It possesses biological activities that are cytosolic and transcription independent. Data have demonstrated that p53 mutants lacking a transactivation domain can induce apoptosis (Kakudo et al., 2005), and activation of p53 in the absence of a nucleus also triggers apoptosis (Chipuk et al., 2003), demonstrating that cytoplasmic p53 can induce apoptosis through a transactivation-independent mechanism. The transcription-independent p53-death pathway couples the nuclear and extranuclear actions of p53. In unstressed cells, cytosolic p53 is sequestered into an inactive complex by soluble cytosolic bcl-XL (B cell lymphoma–extra large). In response to stress, nuclear p53

transactivates its target gene *PUMA* (*p53 up-regulated modulator of apoptosis*), which liberates p53 to activate monomeric Bax (Bcl-associated X) in the cytosol (Chipuk et al., 2005).

Upon exposure to apoptotic stimuli, total cellular levels of p53 rapidly stabilize and a fraction accumulates at the mitochondria, where it controls a direct apoptotic program. Induced p53 rapidly translocates to the outer membrane of mitochondria, where it engages in inhibitory and activating complexes with the anti- and proapoptotic members of the Bcl-2 family of mitochondrial permeability regulators (bcl-XL/bcl-2 and BAK [BCL2-antagonist/killer], respectively). This translocation precedes changes of mitochondrial membrane potential, cytochrome *c* release, and caspase activation, which induces outer membrane permeabilization and the release of apoptotic activators (Sansome et al., 2001; Mihara and Moll, 2003; Arima et al., 2005; Nemajerova et al., 2005; Moll et al., 2006). Mitochondrial translocation of endogenous WT-p53 occurs both in vitro and in vivo in response to various p53-activating cellular stresses in different cell types (Sansome et al., 2001; Mihara and Moll, 2003; Arima et al., 2005; Moll et al., 2006). A recent study of melanocytes demonstrated translocation of p53 to the mitochondria upon UVA irradiation but not UVB (Wäster and Ollinger, 2009).

The targeting of p53 to the mitochondria has received considerable interest. There is no reported mitochondrial translocation motif within the p53 polypeptide sequence, and N- and C-terminal phosphorylation/acetylation modifications play no major role in mitochondrial targeting of p53 (Nemajerova et al., 2005). Evidence suggests that monoubiquitinylation of p53 provides a trafficking signal that redirects the cell from a fate of degradation and inactivation in unstressed cells to mitochondrial translocation and activation early during the stress response (Marchenko et al., 2007). Nuclear export of p53 is not necessary for mitochondrial translocation upon DNA damage, and instead distinct nuclear and cytoplasmic p53 pools become simultaneously and rapidly stabilized after genotoxic stress.

There is significant evidence to support a role for *TP63* in carcinogenesis, and the tissue-specific expression of isoforms warrants exploration of this p53 family member in melanoma. To date, expression or function of *TP63* in melanoma has not been systematically investigated. This study demonstrates a biological role for *TP63* in melanoma through a dual mechanism of negative regulation of apoptosis: through translocation of p63 to the mitochondria with consequent impact on expression of the BCl2 family proteins and through derepression of p53 in the nucleus. By identifying a functional interaction between TP63 and TP53, we provide a possible explanation for the notorious chemoresistance observed in melanoma.

RESULTS

p63 is expressed in melanoma cell lines and melanoma tissue samples

Primers designed to detect all splice variants of *TAp63* (Koga et al., 2003) and *ΔNp63* (Yang et al., 1998) were used to determine cellular expression in the skin. Both *TA* and *ΔN p63* isoforms were expressed in samples obtained from different body sites from a range of skin phototypes (Fig. 1 A). TAp63 and ΔNp63 were expressed in keratinocytes; the relative expression was in keeping with a previous study (Senoo et al., 2007). *TAp63* but not *ΔNp63* was also expressed in fibroblasts. RT-PCR analysis failed to detect expression of either isoform in primary melanocyte cultures, but both isoforms were expressed in a metastatic melanoma cell line (WM1158). Despite the apparent lack of *TP63* expression in primary melanocytes, quantitative PCR (Q-PCR) demonstrated significant up-regulation of *TP63* in 24/33 (73%) melanoma cell lines (Fig. 1 B). No correlation was observed between expression of either *TAp63* and/or *ΔNp63* with $BRAF^{V600E}$ mutation or *NRAS* mutation status ($P > 0.05$, Fisher's exact test). In general, up-regulation of the two isoforms of *TP63* was mutually exclusive with simultaneous up-regulation occurring infrequently (18%; $n = 6$). Western blotting data confirmed differential expression of p63 protein in melanoma cell lines compared with primary melanocyte cultures (Fig. 1 C).

Analysis of whole genome microarray data in melanoma tissue samples by Scatolini et al. (2010) revealed up-regulation of *TP63* at all stages of melanoma progression but no significant up-regulation of *TP53* or *TP73* (Fig. 1 D). Immunohistochemical expression of p63 was investigated in 40 primary melanoma tissue samples in a melanoma tissue microarray (mTMA; Biomax). Overall, 16/40 (40%) samples in the mTMA demonstrated strong labeling of p63 and costaining with HMB-45 (human melanoma black-45), confirming expression of p63 in melanoma cells; two examples are shown in Fig. 1 E. Statistical analysis of clinical data available for the melanoma tissue array samples demonstrated no significant demographic differences between p63-positive and -negative melanomas (Table S1).

p63 is responsive to DNA-damaging agents in melanoma and relocates to the mitochondrial compartment

Primary melanocyte cultures were treated with UVB radiation and various chemotherapeutic agents (cisplatin, etoposide, and doxorubicin) from 6 to 48 h (Fig. 2 A and not depicted). No stabilization or reactivation of p63 was observed in melanocyte cultures despite induction of DNA damage and induction of an apoptotic pathway. Upon DNA damage, up-regulation of both nuclear and cytoplasmic p63 was observed in 8/9 (88%) established melanoma cell lines, with stabilization occurring as early as 2 h and in some cell lines persisting for 48 h (not depicted). Stabilization of the p63 gene and protein was demonstrated in established melanoma cell lines treated with various DNA-damaging agents (Fig. 2, C and D). No induction of p63 was observed upon treatment with dacarbazine (not depicted). Treatment with novel BRAF inhibitors (PLX4032 and PLX4720) affected p63 expression in a cell line–specific manner with stabilization of p63 in some cases (Fig. 2, E and F).

Cytoplasmic stabilization of p63 in melanoma cell lines led to investigation of relocation of p63 to different subcellular compartments. MitoTracker Orange was used as a marker of mitochondria to investigate localization of extranuclear p63

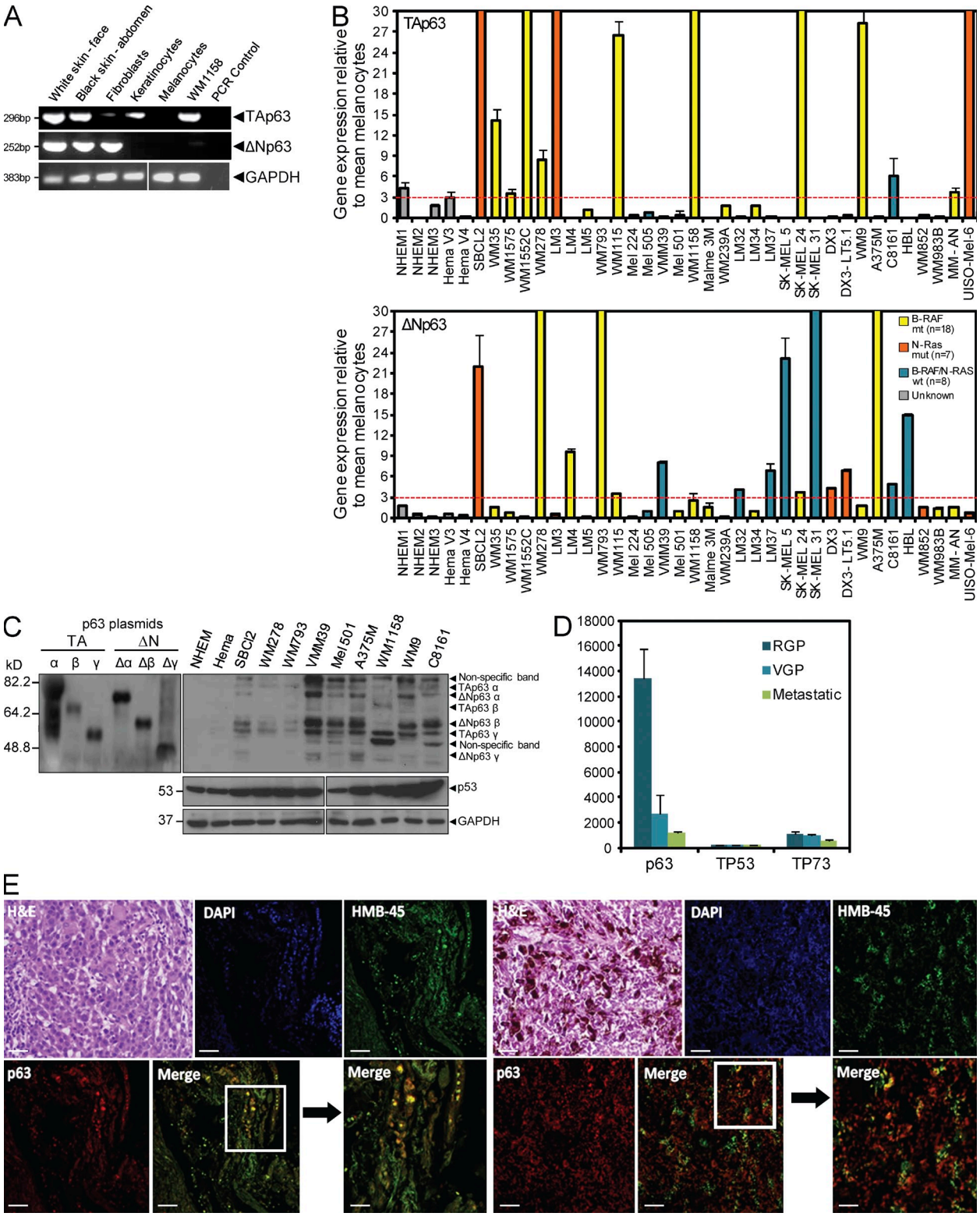

Figure 1. p63 is expressed in melanoma cell lines and melanoma tissue samples. (A) TP63 expression in human normal skin cellular components (RT-PCR). Controls included omission of cDNA. GAPDH was used as a loading control. (B) Q-PCR of *TAp63* (39%, 13/33; top) and *ΔNp63* (51%, 17/33; bottom) in panel of established primary melanoma and metastatic melanoma cell lines. The bars show the folds of p63 mean expression ± SD compared with mean expression of *TP63*/*GUS* in five primary melanocyte cultures (NHEM1, NHEM2, HEMa 3, HEMa V3, and HEMa V4). Measurements have been performed at least three times for each cell line at different passages. Dotted lines mark threefold increase in gene expression compared

upon DNA damage. In untreated melanoma cells, localization of p63 is largely confined to the nucleus (Fig. 2 E), but upon treatment with paclitaxel (as early as 3 h) stabilization of p63 was observed in the cytoplasm and, more specifically, in the mitochondria, as demonstrated by colocalization with MitoTracker Orange (Fig. 2 G). Similar effects were observed in melanoma cells treated with doxorubicin and etoposide (not depicted). Collectively, these data confirm that p63 is up-regulated in response to genotoxic stress and is localized to both nuclei and mitochondria.

Subcellular fractions of melanoma cell protein lysates were analyzed using Western blotting to enrich for proteins of interest within mitochondrial and nuclear fractions. Purity was confirmed by incubation with anti–Lamin A (nuclear), anti-mtHsp70 (mitochondrial heat shock protein 70; mitochondrial), and anti-GAPDH (cytosolic) antibodies. In untreated WM1158 cells, TAp63α was largely expressed in the nuclear fraction, whereas TAp63γ was largely expressed in the mitochondrial compartment, with up-regulation of each isoform in their respective compartments in response to chemotherapeutic agents (Fig. 2 H). Results showed predominant p53 stabilization in the nucleus, with less pronounced stabilization in mitochondria (Fig. 2 H). In support of this, immunofluorescence microscopy of the same cells confirmed nuclear stabilization upon DNA damage treatment, suggesting that in melanoma cells, p53 also displays nuclear stabilization in response to genotoxic stress with possible translocation to the mitochondria (not depicted). In A375M cells, ΔNp63α and ΔNp63β were stabilized in nuclear and mitochondrial compartments upon treatment (not depicted).

Immunogold localization of protein using transmission electron microscopy was used to determine the exact location of p63 within mitochondria. Treated A375M and WM1158 cells were pelleted, fixed, and processed for transmission electron microscopy. Mitochondria were identified by their characteristic ultrastructure and confirmed by the presence of immunogold particles secondary to anti-mtHsp70 antibody (Fig. 2, I and J). Upon treatment with paclitaxel, immunogold particles of p63 were demonstrated in the nucleus and the mitochondria of both cell lines using various anti-p63 antibodies (Fig. 2, I and J). No association of immunogold particles with other subcellular structures identified by their characteristic ultrastructure, e.g., the Golgi body, was observed (not depicted). These data suggest that upon genotoxic stress, p63 translocates between the nucleus, cytoplasm, and mitochondrial compartments to exert its function.

Fractionation using a novel flow cytometry technique can quantify relative p63 protein translocation to subcellular compartments

Subcellular fractionation enriches for p63 protein within each fraction but does not allow for assessment of changes in concentration of p63 in response to genotoxic stress. To quantify the relative concentration of p63 in different cellular compartments, a new method recently developed in our laboratory was used as an alternative to the fractionation technique (summarized in Materials and methods and Fig. 3 A; Leverrier et al., 2007).

A375M cells were treated with etoposide in a time-dependent manner to establish the kinetic profile of p63 expression using flow cytometry (Fig. 3 A). To quantify the degree of p63 stabilization upon treatment, the percentage of positive events was combined with the relative fluorescent intensity of the Cy5 signal. Expression of p63 was determined by comparing the expression of p63 with the IgG mouse isotype control for each treatment. The relative concentration of p63 in treated A375M cells (considered total p63) and in fractionated cells in the nuclei and mitochondria was calculated by comparing concentration of p63-Cy5 in each fraction for each treatment with the untreated sample (Fig. 3 A). Histograms demonstrate stabilization of total p63 to a maximum at 6 h with a reduction thereafter to 24 h (Fig. 3 A, i and ii). When cells were lysed and reanalyzed (Fig. 3 A, iii and iv), expression of nuclear p63 linearly increased to a maximum at 24 h, whereas the stabilization profile of mitochondrial p63 reflected that of total p63 (Fig. 3 A, iii and v).

Flow cytometry experiments confirmed stabilization of p63 in both nuclear but to a greater extent in the mitochondrial compartment in other fractionated melanoma cell lines, including WM1158 (metastatic melanoma) and SBCl2 (primary radial growth phase [RGP] melanoma) cells, upon treatment with cisplatin, etoposide, and paclitaxel compared with untreated samples (Fig. 3, B and C; and not depicted). The purity of the subcellular fractions was confirmed using confocal microscopy (Fig. 3, D and E).

Posttranslational modifications, e.g., phosphorylation, of p63 are reported to significantly alter protein levels (Osada et al., 1998; MacPartlin et al., 2005; Westfall et al., 2005; Suh

with mean expression in melanocyte cultures. GUS was used as an endogenous control. (C) 80 µg protein lysates from primary melanocyte cultures (NHEM and Hema) and melanoma cell lines probed for p63 (using anti-p63 antibody AB-4 which detects all isoforms of p63). GAPDH was used as loading control. (D) Analysis of mean expression ± SD of *TP53* family genes in melanoma tissue samples using gene microarray (Agilent Technologies; Scatolini et al., 2010). VGP, vertical growth phase; Metastatic, melanoma metastases. (E) Immunofluorescence microscopy demonstrating expression of p63 in primary cutaneous melanomas (mTMA). (left) Primary melanoma from left arm (81-yr-old female). (right) Primary melanoma with heavy melanin deposition from right thumb (62-yr-old female). Panels described left to right, top to bottom: hematoxylin and eosin (H&E) labeling of melanoma, DAPI staining nuclei of melanoma cells, HMB-45 labeling melanoma cells, anti-p63 antibodies (H129/H137) labeling cells within tumor for p63, and merged image demonstrating coexpression of HMB-45 and p63 (yellow). Higher magnification confirms melanoma cells express p63 (yellow). Bars: (H&E thru Merge) 100 µm; (Merge, zoom) 50 µm.

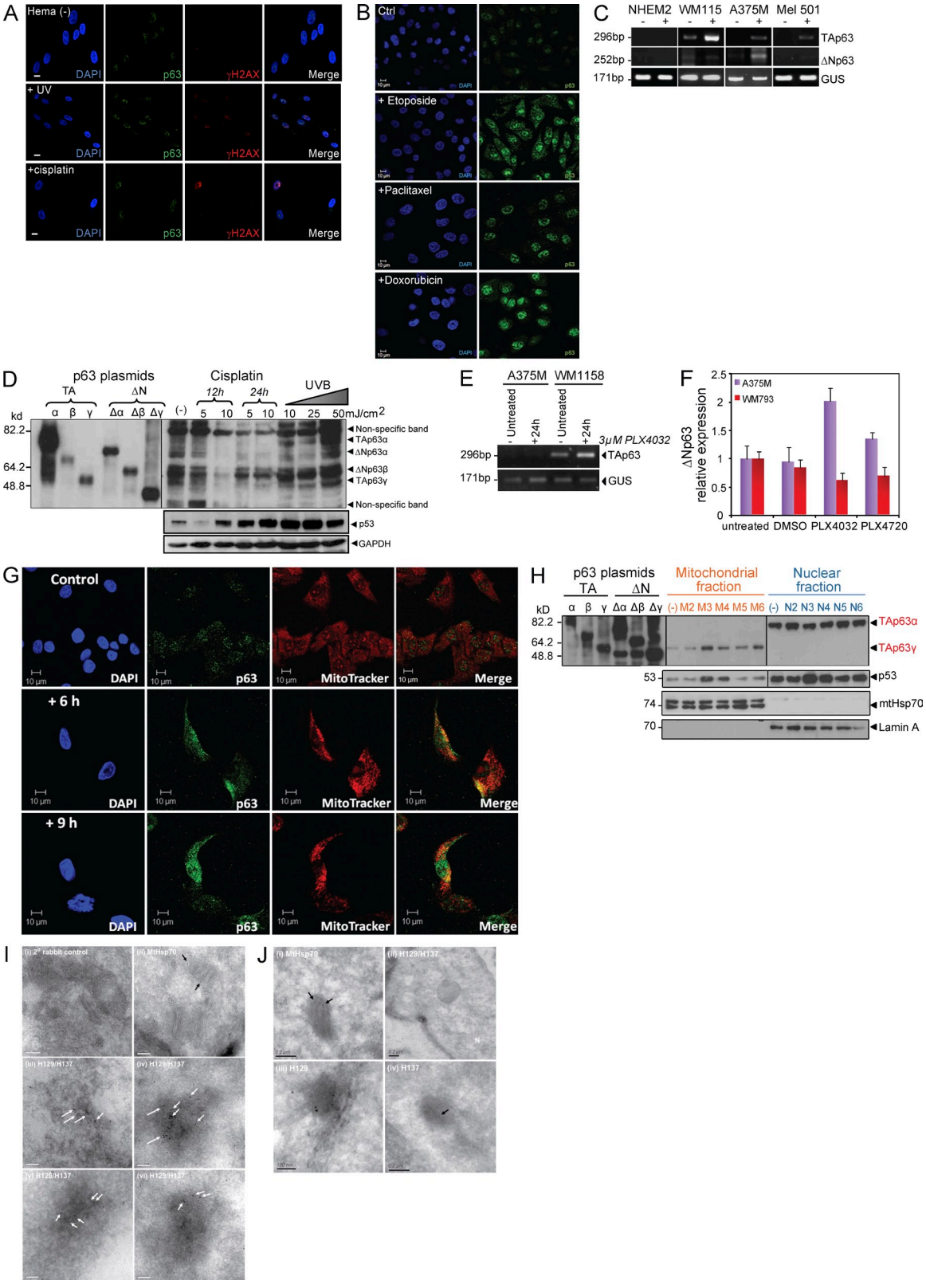

Figure 2. Upon genotoxic stress, p63 is stabilized in melanoma cells and partially relocates to the mitochondria. (A) Immunofluorescence microscopy of untreated melanocytes (Hema V3) and treatment with 50 mJ/cm^2 UVB (for 24 h) or 10 μM cisplatin (for 24 h). Induction of DNA damage and apoptosis assessed using γ-H2AX and cleaved caspase, respectively. DAPI was used to stain nuclei. Images are representative of three independent experiments. (B, top row) Untreated A375M cells contain low levels of endogenous p63 (detected by anti-p63 antibodies H129 and H137), which is largely nuclear.

et al., 2006). Exposure to paclitaxel resulted in up-regulation of total phosphorylated p63 (ser 160/162), which constituted a small fraction of total p63 stabilized, as demonstrated using the flow cytometry fractionation method (Fig. 3 F). Stabilization of phosphorylated p63 was maximal at 90 min and 3 h in the nuclear and mitochondrial fractions, respectively. These data show that in melanoma cells, upon DNA damage, p63 could be phosphorylated in the nucleus before partially relocating to the mitochondria.

Depletion of p63 sensitizes melanoma cells to a mitochondrial apoptotic pathway

Three oligonucleotide sequences were used to silence both TA and ΔN p63 in melanoma cells (Fig. 4 A) to determine the effect on chemosensitivity. The morphology of A375M and WM1158 cells depleted of p63 using three different shRNA-p63 clones was not dissimilar to those stably expressing shRNA-scramble (not depicted). Significant depletion of p63 using all three shRNA-p63 clones (1, 2, and 3) was demonstrated using Q-PCR and Western blotting in WM1158 (Fig. 4 B) and A375M cells (Fig. 4 E). No difference in TAp63 and ΔNp63 mRNA expression was observed between non-transfected melanoma cells and those stably expressing scramble sequences, confirming the shRNA-scramble had no effect on p63 gene expression (Fig. 4, B and E). Depletion of p63 using shRNA clones 1 and 2 in both WM1158 (Fig. 4 C) and A375M cells (Fig. 4 F) demonstrated significantly increased apoptosis upon treatment with etoposide, paclitaxel, and cisplatin, as demonstrated by the Annexin V assay. No effect was observed with dacarbazine, even at increasing doses (Fig. 4, C and F; and not depicted). Treatment with novel BRAF inhibitors (PLX4032 and PLX4720) significantly increased apoptosis of melanoma cells that were depleted of p63 (Fig. 4, I and J).

Upon treatment of WM1158 cells (sh-Ctrl) with etoposide or paclitaxel (16 h), induction of the mitochondrial apoptotic pathway was demonstrated through cytosolic release of cytochrome *c* and up-regulation of Apaf-1 (apoptotic protease-activating factor 1; Fig. 4 D). Western blotting of WM1158 cells treated with various chemotherapeutic agents demonstrated significant stabilization of total and phosphorylated p53 (ser-15), MDM2 (mouse double minute 2), and MDM4 in p63-depleted cells (Fig. 4 G). In addition, up-regulation of proapoptotic BCL2 proteins such as Bax, Bak, and Puma and down-regulation of antiapoptotic factors such as Bcl-xL, Mcl-1 (myeloid cell leukemia 1), and Bcl-2 were detected in sh-p63 cells exposed to cisplatin, etoposide, or paclitaxel (Fig. 4 G). Among the down-regulated antiapoptotic factors, Bcl-xL was consistently down-regulated by all the treatments in the absence of p63, whereas Mcl-1 expression was significantly decreased only by paclitaxel, which is reported to phosphorylate Bcl-2 (Yamamoto et al., 1999). A similar pattern of expression was also observed in A375M cells upon treatment with paclitaxel (Fig. 4 H), supporting a role for p53 and its downstream targets in the chemosensitivity conferred by depletion of p63. Treatment with BRAF inhibitors (PLX4032 and PLX4720) inhibited phosphorylation of BRAF downstream targets, e.g., phosphorylated ERK (extracellular signal-regulated kinase; P-ERK) and P-MEK (mitogen-activated protein/ERK),

Significant up-regulation of p63 (green) in both nuclear and cytoplasmic compartments of A375M cells was observed upon treatment with 20 µM etoposide (second row), 2 µM paclitaxel (third row), and 2 µM doxorubicin (bottom row) for 6 h. DAPI was used to stain nuclei (blue). Images are representative of three independent experiments. (C) RT-PCR demonstrating up-regulation of TA and/or ΔN p63 expression in three melanoma cell lines, but not melanocytes upon treatment with 10 µM cisplatin for 24 h. GUS was used as a loading control. (D) Western blot of A375M cells treated with cisplatin and UVB. The molecular masses of exogenously transfected p63 plasmids in HEK 293T cells were used to interpret specific p63 isoforms affected by the treatment. Stabilization of both p63 isoforms and p53 demonstrates a dose-dependent effect. (E) RT-PCR of TAp63 in A375M and WM1158 cell lines treated with 3 µM PLX4032 for 24 h. GUS was used as housekeeping gene for mRNA standardization. (F) Q-PCR of ΔNp63 expression in two BRAF mutated melanoma cell lines upon 24-h treatment with 3 µM PLX4032 or PLX4720. GUS was used as an endogenous control. Data show mean expression ± SD for at least three independent analyses performed in duplicates. (G) A375M cells labeled with MitoTracker Orange before treatment with 2 µM paclitaxel and immunofluorescence images shown at 6 and 9 h. DAPI was used to label nuclei. Images are representative of three independent experiments. (H) Western blot of WM1158 cells shows differential subcellular expression of p63 splice variants (TAp63α in the nuclear fraction and TAp63γ in the mitochondrial fraction). This was confirmed by comparing molecular masses with exogenously transfected p63 plasmids in HEK 293T cells (far left six lanes). Treatment with various chemotherapeutic agents, M2/N2 cisplatin, M3/N3 doxorubicin, M4/N4 paclitaxel, M5/N5 etoposide, and M6/N6 UVB, corresponding to mitochondrial (M) and nuclear (N) fractions of the same cells. p53 expression was analyzed using anti-p53 antibody (DO-1), and mtHsp70 and Lamin-A were used as markers for mitochondrial and nuclear protein loading, respectively. Western blot data are representative of cellular fractionation experiments performed in triplicate. (I) Transmission electron micrographs of immunogold labeling of p63 in mitochondria in A375M cells. Mitochondria are characterized by double membrane and cristae projections. (i) Negative control to confirm specificity comprises exclusion of primary antibody. (ii) Mitochondrion confirmed by electron-dense matrix surrounded by double membrane with cristae projections showing immunogold-labeled mtHsp70 localization within the mitochondrial matrix (black arrows). (iii–vi) Electron-dense mitochondria characterized by remarkably electron-dense mitochondrial matrix and cristae. Images demonstrate immunogold localization of p63 (using combination of anti-p63 antibodies H129 and H137) in cytosol, on mitochondrial membranes, and within mitochondrial matrix (white arrows). (J) Transmission electron micrographs of immunogold labeling of p63 in mitochondria (WM1158 cells). (i) Mitochondrion visualized by electron-dense matrix surrounded by double membrane with cristae projections showing immunogold-labeled mtHsp70 localization within the mitochondrial matrix (black arrows). (ii) Nuclear (labeled N) and extranuclear localization of p63. (iii) Electron-dense mitochondria characterized by electron-dense mitochondrial matrix and cristae. Image demonstrates immunogold localization of p63 (using combination of anti-p63 antibody H129) in transit to mitochondria and within mitochondrial matrix. (iv) Electron micrograph showing immunogold labeling of p63 (using H137 anti-p63 antibody) within electron-dense mitochondrion matrix (arrow), and cristae are visible. Images are representative of three independent experiments. Bars: (A, B, and G) 10 µm; (I [i–iii and v] and J [iii]) 100 nm; (I, iv and vi) 200 nm; (J, i, ii, and iv) 0.2 µm.

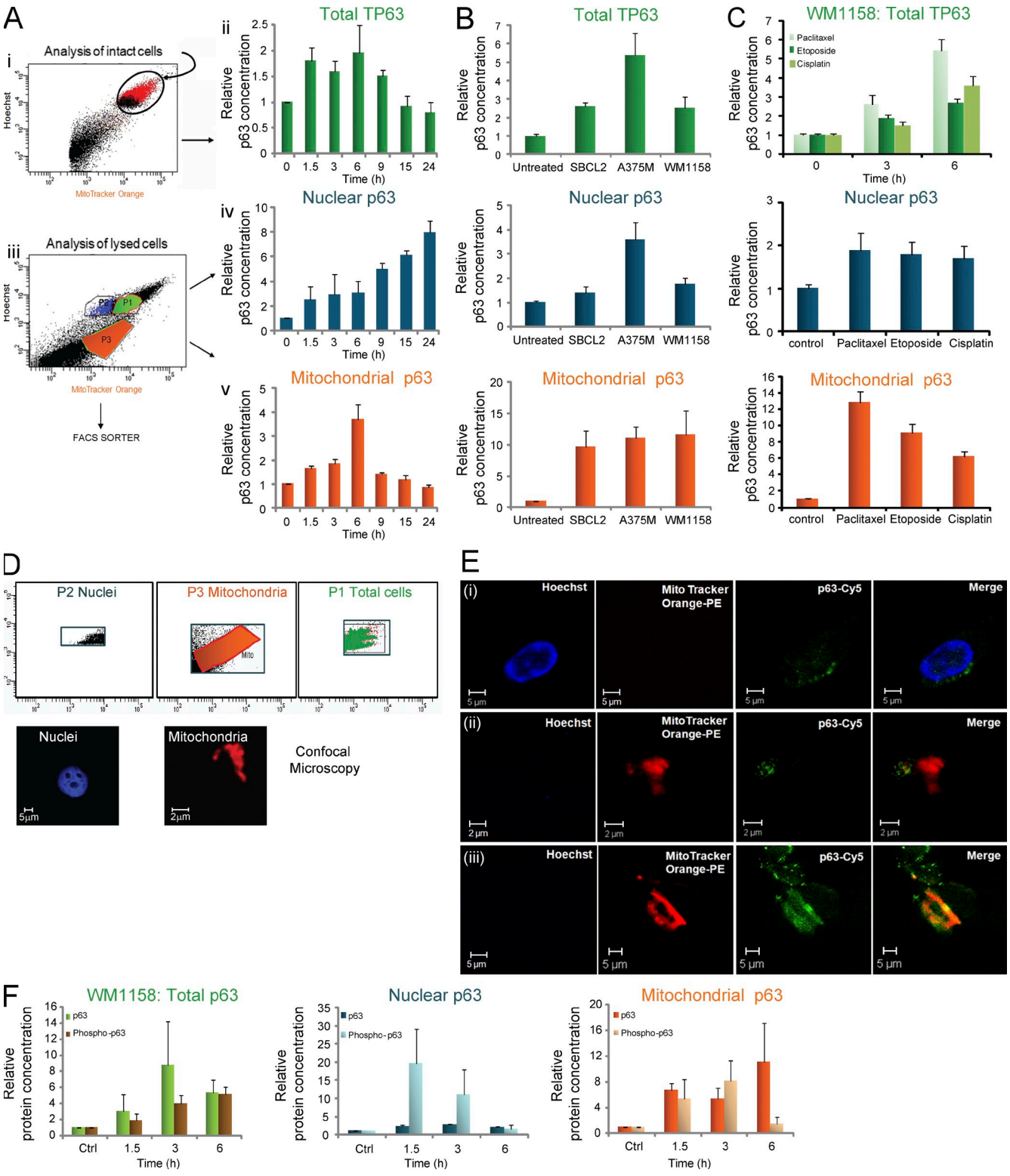

Figure 3. Flow cytometry fractionation technique quantifies p63 translocation to subcellular compartments. (A) Kinetic profile of relative changes in p63 expression upon treatment with etoposide. (i) Scatter plot demonstrating intact A375M cells analyzed for p63-Cy5 expression in whole cells upon treatment with etoposide from 0 to 24 h. Antibody used in flow cytometry experiments detects all isoforms of p63. In A375M cells, the predominant isoform is ΔNp63. (ii) Histogram demonstrates time course of up-regulation of total p63 in A375M cells. (iii) Scatter plot demonstrates analysis of lysed cells and gating of subcellular fractions (P1, whole cells; P2, nuclei; P3, mitochondria). (iv and v) Histograms demonstrating that up-regulation of p63-Cy5 in the nuclear fraction increases linearly after up to 24 h of treatment with etoposide (iv), whereas up-regulation of p63-Cy5 in the mitochondrial

whereas expression levels increased in those cells depleted of p63 (Fig. 4 K). Moreover, p53 was phosphorylated (at ser-15) in p63-depleted cells upon treatment with BRAF inhibitors, together with partial reduction in MDM2 expression and significant reduction in levels of MDM4.

Endogenous p63 prevents p53 nuclear stabilization and requires p53 to translocate into the mitochondria after DNA damage

Induction of p53 downstream targets and the mitochondrial apoptotic pathway raise the possibility that p63 may substitute for or affect the apoptotic function of WT-p53 in melanoma. Flow cytometry fractionation experiments were used to delineate the relationship between p53 and p63, using melanoma cells depleted from p53 (si-p53 A375M cells). MDM2 expression wasn't affected in these cells although the expression of MDM4 significantly increased by depletion of p53 (Fig. 5 A, top). When comparing these melanoma cells with the parental cell line expressing WT-p53 (A375M), upon treatment with paclitaxel or etoposide, significantly greater total (Fig. 5 A), nuclear (Fig. 5 B), and mitochondrial p63 (Fig. 5 C) were observed in the WT-p53 melanoma cell line (A375M), suggesting that translocation of p63 to the mitochondria is dependent on the presence of p53. This was also further confirmed in p53-null melanoma cells (UISO-Mel-6) expressing mainly TAp63 isoform (Fig. 1 B). Upon treatment with paclitaxel, stabilization of TAp63 was predominantly observed in the nuclei (not depicted). Flow cytometry analysis demonstrated up-regulation of total p63 protein levels upon treatment with limited stabilization in either nuclear or mitochondrial fractions (not depicted). Using the same flow cytometry quantification method, significantly greater stabilization of total and nuclear p53 was observed in A375M sh-p63 cells compared with A375M sh-scramble cells upon treatment with etoposide or paclitaxel (Fig. 5 D, left and middle). In contrast, depletion of p63 significantly decreased translocation of p53 to the mitochondria (Fig. 5 D, right). These data suggest that translocation of p53 to the mitochondria may require p63, but more importantly, p63 physiologically prevents p53 nuclear stabilization in melanoma cells. Western blotting of nuclear extracts from A375M cells depleted of p63 after treatment with paclitaxel confirmed significant up-regulation of p53, particularly the phosphorylated forms at ser-15 and ser-46 (the latter reported to link p53 with induction of apoptosis [Oda et al., 2000]), suggesting that up-regulation of p53 in the nucleus results in induction of the mitochondrial apoptotic pathway (Fig. 5 E). Moreover, immunoprecipitation with specific anti-p53 antibody in untreated A375M cells provides evidence of the endogenous interaction with p63 in melanoma cells (Fig. 5 F).

p63 reactivity in primary melanomas is a significant predictor of poorer outcomes

Immunohistochemistry of benign and malignant melanocytic lesions was undertaken to determine the effect of p63 reactivity on patient outcomes. Initially, paraffin-embedded samples of 31 benign intradermal nevi in 17 individuals (6 males and 11 females) were analyzed for p63 expression (using H129 anti-p63 antibody). Mean age at diagnosis was 50.1 yr (range 33.9–70.2 yr). Positive internal control labeling of epidermal keratinocytes with p63 was used for specificity of staining. Overall, positive labeling of p63 in neval melanocytes was demonstrated with low frequency (3/31; 3.2%).

Overall, 81 paraffin-embedded primary cutaneous melanoma tissue samples from 80 individuals were analyzed for expression of p63. Mean age at diagnosis for primary melanomas was 58.4 yr (range 20.7–87.1 yr), male/female ratio was 1:1.3, and median follow up was 4.0 yr (range 0.1–15.3 yr). The mean Breslow thickness was 3.1 mm (range 0.2–13.5 mm). Overall, 47/81 (58%) primary melanoma tissue samples demonstrated positive labeling for p63 (Fig. 6 A). Statistical analysis revealed no significant association between p63 expression

fraction occurs rapidly within 6 h (v). Data show mean expression of p63 ± SEM for three independent experiments performed in triplicate. (B) Histograms demonstrating effect of treatment with etoposide (6 h) in melanoma cell lines (A375M, WM1158, and SBCl2). Total p63 (top), nuclear stabilization (middle), and mitochondrial stabilization (bottom) of p63-Cy5 after treatment with etoposide using flow cytometry fractionation technique. (C) Histograms demonstrating relative changes in p63 expression using flow cytometry fractionation technique after treatment with paclitaxel, cisplatin, and etoposide in WM1158 cells. Antibody used in flow cytometry experiments detects all isoforms of p63. In WM1158 cells, the predominant isoform is TAp63. Total p63 levels stabilize in a time-dependent manner (top), nuclear stabilization of p63 is observed in WM1158 cells with all treatments (middle), and significantly greater mitochondrial p63 is stabilized in response to genotoxic stress (bottom). Data show mean protein expression ± SEM for at least three independent experiments performed in duplicate. (D) Validation of flow cytometry fractionation technique. A375M cells were labeled as outlined and homogenized before analysis using the FACSAria cell sorter. Gated fractions include whole cells, nuclei, and mitochondria that were subjected to FACS and then reanalyzed demonstrating purity of nuclear, mitochondrial, and whole cell fractions. Background noise signal derived from buffers (PBS and Hepes) was excluded. Nuclear and mitochondrial cell fractions were then visualized using confocal microscopy, confirming once again purity of the sorted fraction. Image examples provided are from one of five independent experiments performed. (E) p63-Cy5 expression in cellular fractions obtained from FACS of labeled A375M cells. Cells were labeled with fluorescence markers for nuclei (Hoechst) and MitoTracker Orange (mitochondria) and p63-Cy5 to label p63 in A375M cells. Confocal microscopy analysis demonstrates p63-Cy5 expression in pure nuclear (i) and mitochondrial (ii) fractions of A375M cells. (iii) Giant mitochondria show colocalization (yellow) of p63-Cy5 and MitoTracker Orange, confirming validity of the flow cytometry method of quantification of p63 translocation to the mitochondria. Images are representative of five independent experiments. (F) Comparison of total p63-Cy5 and phosphorylated p63 assessed in intact cells upon treatment with 2 µM paclitaxel. Kinetic analysis of subcellular lysates for phosphorylated p63 after homogenization in nuclei (middle) and mitochondria (right) demonstrate nuclear stabilization of phosphorylated p63 in response to paclitaxel as early as 1.5 h. Data show mean protein expression ± SEM for at least three independent experiments performed in duplicate.

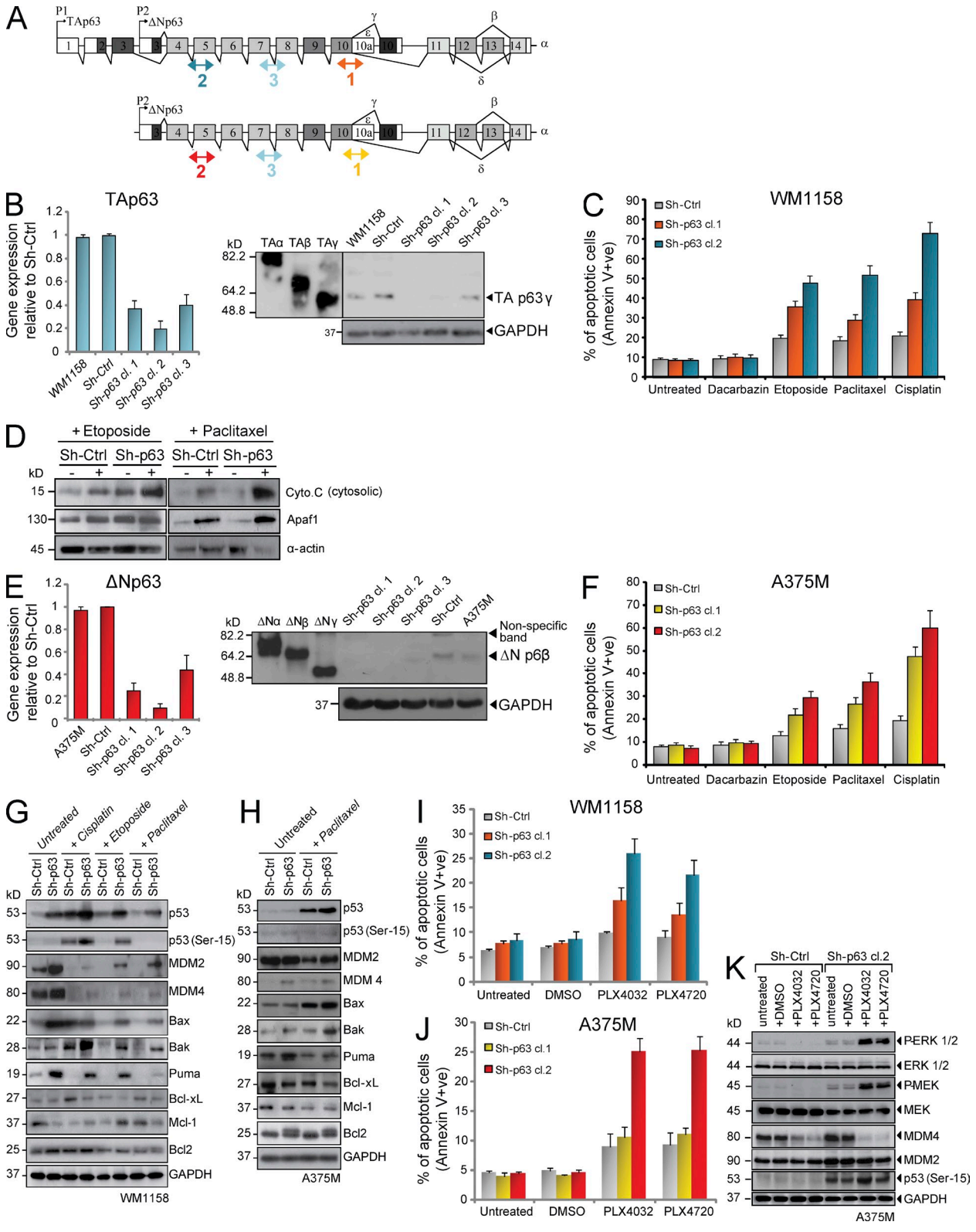

Figure 4. Depletion of p63 by shRNA-p63 clones increases chemosensitivity. (A) Pictorial representation of TAp63 (top) and ΔNp63 (bottom) genes demonstrating targeted sequences used by various RNAi oligonucleotides (1, 2, and 3) designed to target regions in both TA and ΔN isoforms of p63. (B) Q-PCR (left) and Western blot (right) demonstrating knockdown of TAp63 gene and protein achieved in three shRNA-p63 clones. GUS was used as endogenous comparator for Q-PCR and GAPDH for Western blot. Data show mean ± SD of three independent experiments. (C) Percentage of apoptotic cells (Annexin V positive) displayed as mean ± SEM for three independent experiments performed in duplicate. Apoptosis in WM1158 shRNA-p63 cells

of primary tumor with age at diagnosis, gender, or site of melanoma (Table S2). Analyses of histopathological prognostic factors demonstrated significant correlation with Breslow thickness (P = 0.03) but no other features (e.g., histological classification, growth phase, ulceration status, regression, and mitotic rate; Table S2).

For these primary tumors, the mean time to recurrence (n = 7) was 1.60 yr (range 0.04–6.02 yr). Univariate and multivariate analysis demonstrated a trend toward increased recurrence rates in p63-positive tumors but a nonsignificant association (P = 0.197, Wald test; not depicted). Mean time to first metastasis in this cohort (n = 30) was 1.44 yr (range 0.1–4.69 yr). Univariate and multivariate analysis demonstrated an upward trend toward increased metastatic rates in the p63-positive cohort but failed to reach significance (P = 0.105, Wald test; not depicted).

Overall mortality rate for the primary melanoma cohort was 33% (n = 26), and melanoma-specific mortality was 21% (n = 17). Median time to death was 2.6 yr (range 0.5–6.2 yr). Univariate and multivariate analysis using Cox regression analysis for primary tumors demonstrated p63 status to be a significant predictor of worse melanoma-specific outcomes in the univariate analysis (hazard ratio [HR] 3.10; P = 0.04, Cox proportional HR; Table 1 and Fig. 6 B).

p63 reactivity in metastatic melanomas is a significant predictor of poor outcomes

Overall, 19 recurrent melanoma samples and 56 metastatic melanoma tumor samples from 49 individuals (22 males and 27 females) were analyzed. The median age at diagnosis was 60.6 yr (range 30.6–107.6 yr). The median follow up for this cohort was 1.52 yr (range 0.04–8.07 yr). The proportion of p63-positive tumors comprised 10/19 (53%) of recurrent tumors (Fig. 6 C) and 37/56 (66%) of metastatic tumors (Fig. 6 D). Statistical analysis revealed no significant association between p63 expression of metastatic tumor with age at diagnosis, gender, or site of metastasis (Table S3).

Overall mortality for recurrent and metastatic tumors was 45% (n = 22), and melanoma-specific mortality was 37% (n = 18). Median age of death was 62.4 yr (range 30.7–86.7 yr), with median time to death from first recurrence/metastases being 1.25 yr (range 0.08–6.43 yr). Univariate and multivariate analysis using Cox regression analysis for metastatic tumors demonstrated that p63 status was a significant predictor of death from melanoma (multivariate analysis HR 3.86 [1.31–11.39]; P = 0.01; Table 2 and Fig. 6 E).

DISCUSSION

TP63, the master initiator of epithelium stratification, is often dysregulated in cancer progression (Koster et al., 2006; Mills, 2006; Marchini et al., 2008). To date, the expression pattern of p63 isoforms has not been robustly investigated in the melanocyte lineage. Q-PCR analysis, which displays increased sensitivity for detecting low expression levels of isoforms, demonstrated infrequent expression of *TP63* isoforms in primary human melanocyte cultures but significantly elevated expression in >70% of established melanoma cell lines. In contrast with previous immunohistochemistry studies, which showed little or no expression of p63 protein (Brinck et al., 2002; Di Como et al., 2002; Reis-Filho et al., 2003b; Dotto and Glusac, 2006; Bourne et al., 2008; Morgan et al., 2008; Sakiz et al., 2009; Kanner et al., 2010), our data provide the first evidence of marked up-regulation of both p63 mRNA and protein in melanoma cell lines.

In an attempt to characterize the functional role of p63 in melanoma, we demonstrate stabilization of endogenous TA and ΔN p63 isoforms in both nuclear and mitochondrial compartments of melanoma cells in response to genotoxic stress. Depletion of p63 by RNA interference (RNAi) revealed that the expression of TA and/or ΔN p63 isoforms confers resistance to chemotherapy in melanoma cell lines and provides evidence for an oncogenic role of p63 in this tumor. We have demonstrated through immunoprecipitation experiments that p53 and p63 can interact and have shown that stabilization of both p63 and p53 occurs in the nucleus and both are able to translocate to the mitochondria upon genotoxic stress. The mechanism for the latter process appears to be one of codependence, whereby depletion of one protein limits translocation of the other. We propose a mechanism that supports an interaction between p63 and p53 in melanoma cells, whereby depleting p63 results in activation of the p53 mitochondrial apoptotic pathway, rendering melanoma sensitive to both standard chemotherapies and novel BRAF inhibitors. Our data suggest a putative antiapoptotic role for p63 by repression of

compared with shRNA-scramble cells upon treatment with 10 µM cisplatin, 2 µM paclitaxel or 10 µM etoposide, and 200 µM dacarbazine. (D) Western blot of cytosolic fractions of WM1158 upon treatment with paclitaxel or etoposide (16 h) in cells with scramble-shRNA and those depleted of p63 using sh-RNA. (E, left) Q-PCR of cells transfected with three different shRNA-p63 sequences demonstrates significant reduction of ΔNp63 in A375M cells for all three when compared with shRNA-scramble–transfected cells. Data show mean expression ± SD for at least three independent analyses performed in duplicates. (right) Western blot of A375M cells demonstrates significant silencing of ΔNp63 protein levels (the predominantly expressed isoform) by shRNA p63 clones 1 and 2. (F) Percentage of apoptotic cells (Annexin V positive) displayed as mean ± SEM for three independent experiments performed in duplicate. Apoptosis in A375M shRNA-p63 cells compared with shRNA-scramble cells upon treatment with 10 µM cisplatin, 2 µM paclitaxel or 10 µM etoposide, and 200 µM dacarbazine. (G) Protein expression of p53 and selected downstream targets in cells depleted of p63 exposed to cisplatin, etoposide, or paclitaxel treatment. (H) Protein expression of p53 and selected downstream targets in A375M cells depleted of p63 upon treatment with paclitaxel. (I and J) Apoptosis in WM1158 shRNA-p63 (I) and A375M shRNA-p63 (J) cells compared with shRNA-scramble cells upon 24-h treatment with two BRAF inhibitors (3 µM PLX4032 or PLX4720). Percentage of apoptotic cells (Annexin V positive) is displayed as mean ± SEM for three independent experiments performed in duplicate. (K) Protein expression of selected BRAF downstream targets and p53 regulators in A375M cells depleted of p63 upon treatment with 3 µM PLX4032 or PLX4720 for 24 h.

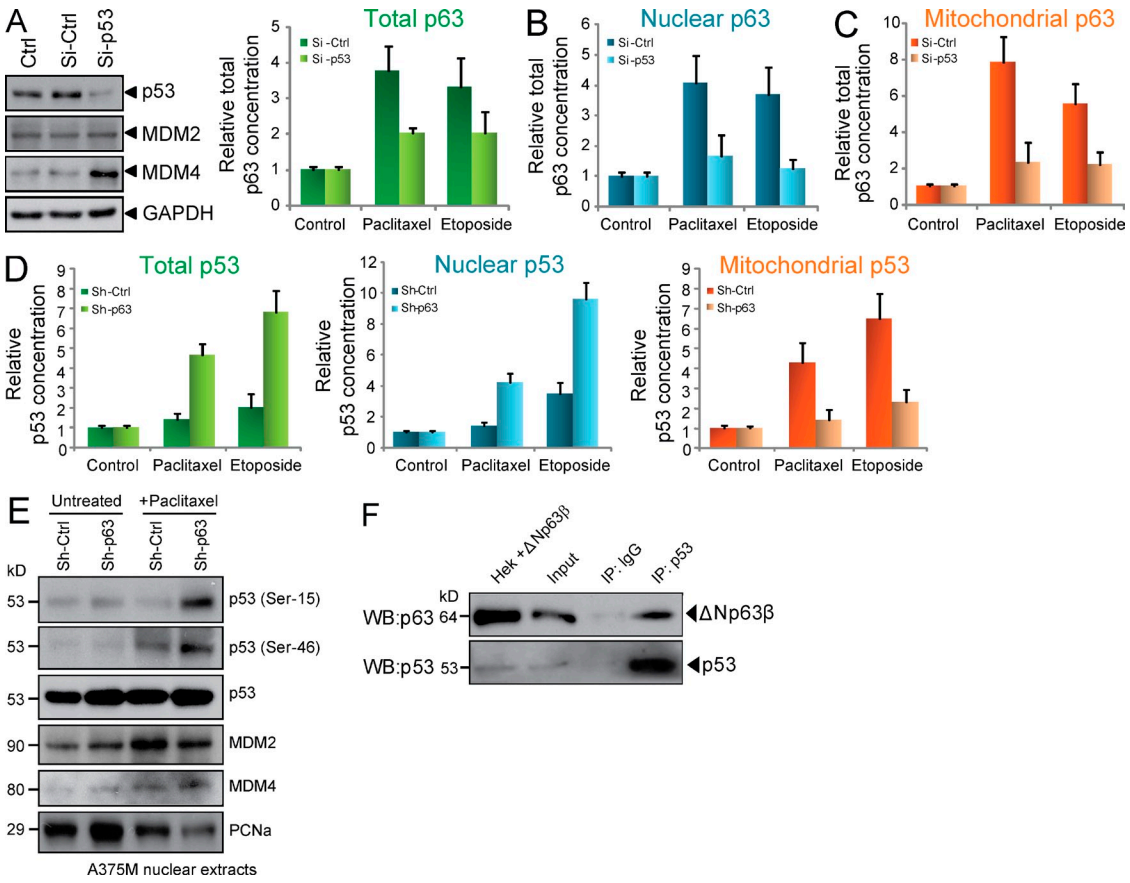

Figure 5. Endogenous p63 prevents p53 nuclear stabilization and requires p53 to translocate into the mitochondria after DNA damage. (A, left) Protein expression of p53, MDM2, and MDM4 in A375M cells depleted of p53 (transient transfection 48 h). GAPDH was used as a loading marker. (right) Profile of relative changes in total p63 expression using flow cytometry fractionation technique in a p53-null melanoma cell line (A375M si-p53) compared with the parental control cell line (A375M si-Ctrl) upon treatment with paclitaxel and etoposide (6 h). (B and C) Comparison of nuclear (B) and mitochondrial (C) p63 protein stabilization in A375M si-p53 versus the parental cell line expressing WT-p53 (A375M si-Ctrl). Data show mean protein expression ± SEM for at least three independent experiments performed in duplicate. (D) Histograms showing relative changes in p53 expression in A375M scramble cells and A375M sh-p63 cells upon treatment with paclitaxel or etoposide (6 h); total (left), nuclear (middle), and mitochondrial (right) p53 in p63-depleted cells compared with scramble-control. (A and D) Data show mean protein expression ± SEM for at least three independent experiments performed in duplicate. (E) Western blot of total and phosphorylated p53, MDM2, and MDM4 derived from nuclear extracts of scramble-A375M cells and sh-p63 cells after treatment with paclitaxel (6 h). PCNA nuclear marker was used as a loading marker. (F) Immunoprecipitation (IP) of endogenous p53 in untreated A375M cells reveals physiological interaction with ΔNp63β. Input: A375M total lysates. HEK293 cells were transfected with ΔNp63 β as a loading marker control. WB, Western blot.

nuclear p53, which may be one explanation for the failure of p53 apoptotic function in melanoma.

To support these findings, we have provided the first evidence that a significant proportion of cutaneous melanoma tumors express p63 protein. These data demonstrate nuclear and cytoplasmic expression of p63 in 40–63% of melanoma tissue samples, depending on stage of disease progression. Analysis of the p63-positive population demonstrated a significant association with Breslow thickness of primary melanoma and a positive trend toward shorter time to recurrence and to metastases. Moreover, individuals with p63-postive primary and metastatic tumors had significantly worse disease-specific outcomes.

This study has demonstrated the endogenous expression of p63 in melanoma cell lines and melanoma tissue samples using a variety of methods and demonstrated a physiological role for this gene in melanoma. Although physical localization of p63 to the mitochondria has not been previously reported, here we have shown using a range of methods (immunofluorescence, electron microscopy, Western blot of subcellular fractionation, and FACS quantification analysis) that translocation of both TA and ΔN p63 to the mitochondria occurs relatively rapidly compared with a more gradual stabilization of the protein in the nucleus, suggesting involvement of p63 in the mitochondrial apoptotic pathway, while still retaining nuclear transcriptional activity. This is the first study to demonstrate p63 relocation to the mitochondria but also to quantify the stabilization in various subcellular compartments using a novel flow cytometry fractionation technique.

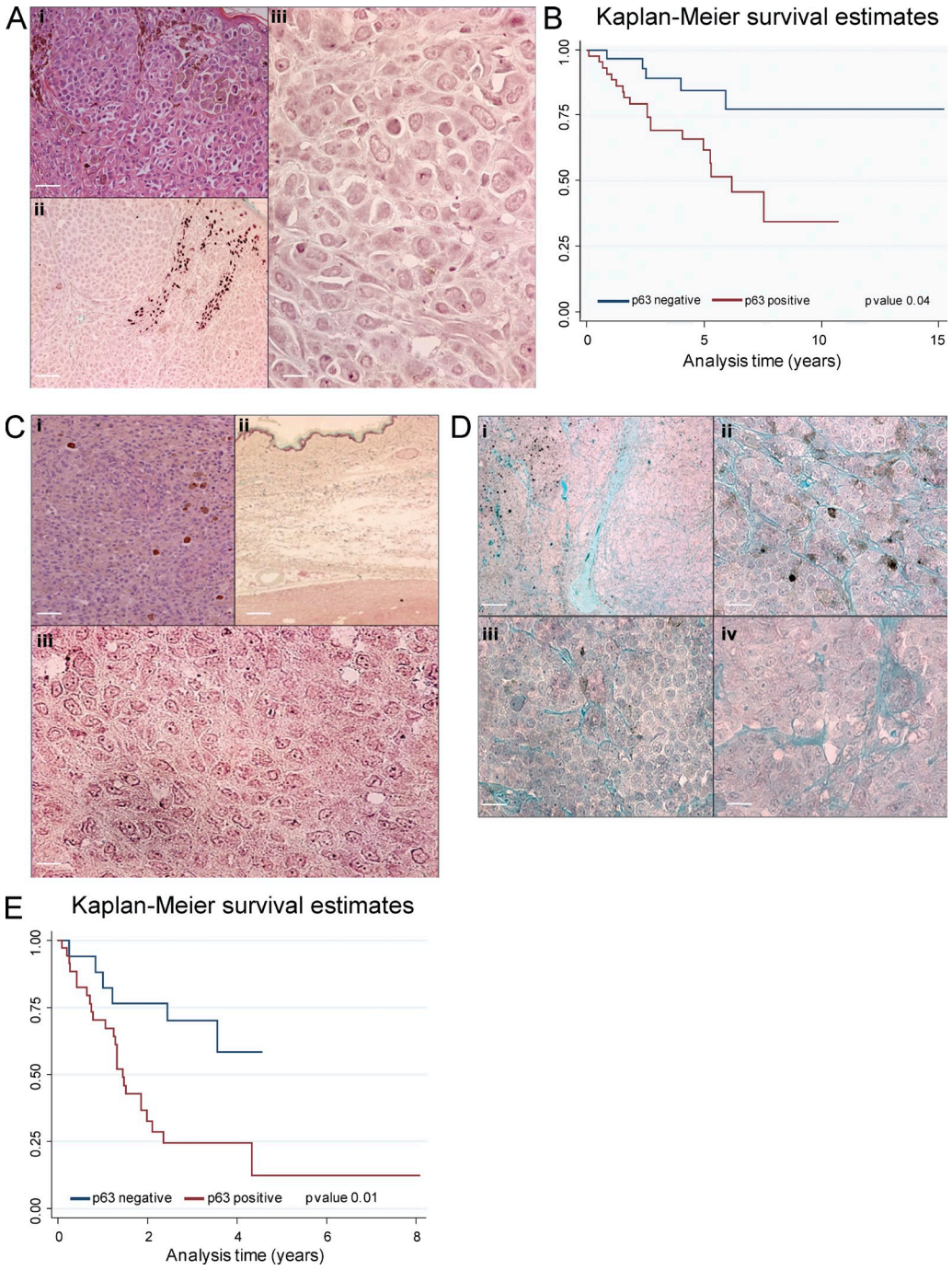

Figure 6. p63 is a novel prognostic indicator in primary and metastatic melanoma. (A) Example of immunohistochemistry of primary melanoma: 36-yr-old male, nonulcerated, superficial spreading melanoma from trunk, Breslow thickness 3.5 mm. (i) Hematoxylin and eosin stain. (ii) Anti-p63 antibody demonstrating strong nuclear labeling of epidermal keratinocytes confirming positive internal control. (iii) Higher magnification of melanoma cells showing nuclear and cytoplasmic p63 reactivity. (B) Kaplan-Meier survival estimates (melanoma specific) in the primary melanoma cohort (n = 81) demonstrate p63 reactivity to be a significant predictor of poorer outcomes (univariate analysis HR 3.10; P = 0.04, Cox proportional HR). (C) Example of recurrent melanoma (72-yr-old male) on arm. (i) Hematoxylin and eosin stain. (ii) Anti-p63 antibody demonstrating strong nuclear labeling of epidermal keratinocytes confirming positive internal control. (iii) Higher magnification confirming both nuclear and cytoplasmic p63 reactivity. (D) p63 reactivity demonstrated in three different lymph nodes completely replaced with metastatic melanoma in an 81-yr-old male. Low (i) and high (ii) magnifications of same node are shown, as well as two other lymph nodes (iii and iv); all three nodes demonstrate nuclear and cytoplasmic labeling of melanoma infiltration. Bars: (A and C [i and ii] and D [i]) 100 µm; (A and C, iii) 30 µm; (D, ii–iv) 50 µm. (E) Kaplan-Meier survival estimates (melanoma specific) in the metastatic melanoma cohort (n = 56) demonstrate p63 reactivity to be a significant predictor of poorer outcomes (multivariate analysis HR 3.86; P = 0.01, Cox proportional HR).

Table 1. Cox regression analysis of melanoma-specific mortality for primary melanoma archival tissue samples

Clinicopathological factors	Univariate analysis		Multivariate analysis	
	HR (95% CI)	P-value	HR (95% CI)	P-value
Age at diagnosis (yr)	1.04 (1.01–1.07)	0.014		
Gender				
Female	1			
Male	1.36 (0.53–3.47)	0.517		
Site of melanoma				
Head/neck	1			
Extremities	0.47 (0.10–2.10)	0.32		
Acral	0.80 (0.13–4.79)	0.806		
Trunk	1.14 (0.31–4.24)	0.847		
Breslow thickness				
T1	1			
T2	-	-		
T3	-	-		
T4	17.30 (2.25–133.27)	0.006		
Clark level				
II	1			
III	3.53 (0.39–31.66)	0.259		
IV	5.04 (0.64–39.88)	0.125		
V	14.29 (1.59–128.58)	0.018		
Histological classification				
ALM	1			
NMM	3.13 (0.41–23.87)	0.27		
SSM	0.44 (0.05–4.25)	0.477		
Growth phase				
RGP	1			
VGP	6.85 (0.91–51.63)	0.062		
Ulceration status				
No	1		1	0.00
Yes	7.25 (2.38–22.12)	0.001	7.04 (2.30–21.50)	
Mitotic rate (number/mm^2)				
Stage 1	1			
Stage 2	1.09 (0.18–6.57)	0.922		
Stage 3	4.63 (1.21–17.69)	0.025		
Stage 4	4.77 (0.79–28.90)	0.089		
Regression				
No	1			
Yes	0.25 (0.03–1.87)	0.176		
Microsatellites				
No	1			
Yes	4.63 (1.73–12.39)	0.002		
Recurrence				
No	1			
Yes	1.50 (0.34–6.57)	0.588		
Metastases				
Nil	1			
Lymph	-	-		
Multiple	-	-		
p63 status				
Negative	1		1	0.074
Positive	3.10 (1.02–9.48)	0.047	2.77 (0.91–8.51)	

ALM, acral lentiginous melanoma; NMM, nodular melanoma; SSM, superficial spreading melanoma; VGP, vertical growth phase. P-values are from Cox proportional HR. For Breslow thickness categories, T1, 0–1 mm; T2, 1–2 mm; T3, 2–4 mm; and T4, >4 mm. Clark level defines depth related to skin structures: level I, melanomas confined to the outermost layer of the skin, the epidermis; level II, penetration by melanomas into the second layer of the skin, the dermis; level III, melanomas invade deeper through the dermis but are still contained completely within the skin; and level IV, penetration of melanoma into the fat of the skin beneath the dermis, penetration into the third layer of the skin, the subcutis. Mitotic rate categories were chosen based on significant survival differences demonstrated between these groupings (Azzola et al., 2003). "-" indicates that there were not enough values in each subcategory to undertake an analysis.

Posttranslational modification analysis of p63 revealed that phosphorylation occurs within 3 h of exposure to genotoxic agents, predominantly in the nucleus but also in the mitochondria. This may affect stability of the protein and/or its transactivation abilities. Phosphorylation of p63 in keratinocytes has no effect on subcellular localization (Westfall et al., 2005), whereas it has been shown recently that phosphorylation of p53 may have a role in targeting the protein to the mitochondria (Nemajerova et al., 2005; Mancini et al., 2009). Based on these data, we speculate that, analogous to p53, phosphorylation of p63 may contribute to the stability of the protein in the nucleus and may also assist in targeting the protein to the mitochondria. Further work is required to characterize targeting of p63 to the mitochondria.

p63 has been linked to chemosensitivity in several tumors: in head and neck squamous cell carcinoma, ΔNp63 was a key determinant of therapeutic response (Rocco et al., 2006), and expression correlated with clinical response to cisplatin (Zangen et al., 2005); in breast cancer, p63 expression positively correlated with chemosensitivity to cisplatin (Rocca et al., 2008); and in hepatoma cells, transfection of TAp63α sensitized cell lines to chemotherapy and transient depletion led to chemoresistance (Gressner et al., 2005). Studies have reported p63 to be a biomarker for poor prognosis and cancer progression in breast cancer and follicular cell lymphoma, respectively (Ribeiro-Silva et al., 2003; Fukushima et al., 2006). Although p63 has been reported to primarily be a nuclear protein (el-Deiry et al., 1995; Dellavalle et al., 2001; Di Como et al., 2002), aberrant cytoplasmic expression is reported in lung and prostate cancers (Narahashi et al., 2006; Dhillon et al., 2009) and was associated with increased prostate cancer–specific mortality, reduced apoptosis, and higher proliferative activity, suggesting an oncogenic role in prostate cancer progression and survival (Dhillon et al., 2009). Our data support these findings in melanoma. The heterogeneity of this cancer raises the possibility that such a finding could provide a novel therapeutic approach aimed at counteracting p63 expression in melanoma cells and consequently sensitizing melanoma to standard chemotherapeutic agents.

Our data propose a physiological interaction between p53 and p63, providing an explanation for the failure of p53-mediated apoptosis in melanoma, in particular in response to chemotherapeutic agents. Although both TA and ΔNp63 isoforms can act as transcription factors when homodimerized, the ΔN isoforms can heterooligomerize with the TAp63 isoforms (as well as with other p53 family members) and modify their activity in vitro (Hibi et al., 2000; Choi et al., 2002; Serber et al., 2002; Chan et al., 2004). This could be a result of heterooligomer formation or co-translocation by molecular chaperones recognized to transport p53, e.g., hsp90 or hsp70 (Walerych et al., 2004, 2009; Whitesell and Lindquist, 2005).

Endogenous p63 prevents nuclear p53 stabilization after a stress response. This effect could be caused by either inhibition of p53 entry into the nucleus or, more likely, an inhibitory effect on stability of p53 through induction of ubiquitin ligases, e.g., MDM2, which is often overexpressed in melanoma and recognized as one of the main causes of p53 inactivity in melanoma cells (Polsky et al., 2002; Muthusamy et al., 2006; Ji et al., 2012). Reactivating p53 to restore its tumor-suppressive capacity has received great attention, with emphasis on reduction of mdm2 to achieve this (Smalley et al., 2007; Gomez-Monterrey et al., 2010; Michaelis et al., 2011; Verhaegen et al., 2012). Recently, elevated expression of MDM4 was demonstrated to be a key determinant of impaired p53 function in melanoma (Gembarska et al., 2012). Although previous in vitro data indicate that both MDM2 and MDM4 could not repress transactivation of p63 isoforms (Little and Jochemsen, 2001), our results suggest otherwise in melanoma. Our data propose a role for p63 in modulating expression of p53, MDM2, and MDM4 through depletion of MDM2 (possibly through degradation) and MDM4, thus increasing p53-mediated chemosensitivity in melanoma. We have demonstrated that depletion of p63 significantly increases nuclear expression of p53 and mdm2 in conjunction with total MDM4 protein levels. Although we cannot definitively confirm whether p63 directly represses MDM2 and MDM4 in addition to p53, or whether this is an indirect effect caused by their feedback

Table 2. Cox regression analysis of melanoma specific mortality for metastatic melanoma archival tissue samples

Clinicopathological factors	Univariate analysis		Multivariate analysis	
	HR (95% CI)	P-value	HR (95% CI)	P-value
Age at diagnosis (yr)	1.03 (1.00–1.07)	0.053	1.03 (1.01–1.06)	0.01
Gender				
Female	1			
Male	1.27 (0.55–2.94)	0.579		
Site of metastatic melanoma				
Lymph node	1		1	
Other sites[a]	1.95 (0.86–4.41)	0.108	2.29 (1.10–4.75)	0.026
p63 status				
Negative	1		1	0.014
Positive	3.27 (1.08–9.87)	0.035	3.86 (1.31–11.39)	

P-values are from Cox proportional HR.
[a]Skin, lung, parotid, and brain.

loop with p53 (Li et al., 2010), these data support a role for p63 to disrupt the p53–MDM2 and p53–MDM4 axis in melanoma with consequent reactivation of chemosensitivity. We propose that expression of p63 in melanoma might be considered when designing novel targets aimed at disrupting the p53–MDM2 and/or p53–MDM4 interactions.

In summary, we have demonstrated the first evidence of a biological role for p63 in melanoma cells supporting preferential up-regulation of TP63 over p53 mutations, whereby p63 acts to negatively regulate p53 function. In response to DNA damage, p63 is stabilized in the nuclei and translocates to the mitochondria where it acts to repress apoptosis through direct and indirect inhibitory function on proapoptotic effectors in the p53 apoptotic pathway. These data unexpectedly implicate both TA and ΔN p63 isoforms in mediating chemoresistance in melanoma and impact novel therapeutic strategies used to treat melanoma.

MATERIALS AND METHODS

Cell lines

33 established melanoma cell lines and 8 human primary melanocytes cultures were profiled (Tables S4 and S5). Human melanoma cell lines WM35, WM1575, WM1552C, WM793, WM115, WM278, WM1158, WM9, WM852, WM983B, and WM239A were donated by M. Herlyn (Wistar Institute, Philadelphia, PA). SBCl2 RGP-like cells were a gift of B.C. Giovanella (Stehlin Foundation for Cancer Research, St. Joseph Hospital, Houston, TX). LM3, LM4, LM5, LM32, LM34, and LM37 were provided by M. Rodolfo (Fondazione IRCCS Istituto Nazionale Tumori, Milan, Italy). VMM39, Mel 224, Mel 505, Mel 501, SK-MEL 5, and SK-MEL 24 were provided by T. Crook (University of Dundee, Dundee, Scotland, UK). DX3, DX3LT5.1, and A375M were donated by J.F. Marshall (Queen Mary University of London [QMUL], London, England, UK). C8161 cells were a gift from M.J.C. Hendrix (Children's Memorial Research Center, Chicago, IL). SK-MEL 31, HBL, and MALME-3M were provided by J. Vachtenheim (University Hospital Prague, Prague, Czech Republic) and by G.E. Ghanem (University of Brussels, Brussels, Belgium). p53-null MM-AN cells were a gift from B.A. Gilchrest (Boston University School of Medicine, Boston, MA), whereas UISO-mel-6 were provided by T.K. Das Gupta (University of Illinois at Chicago, Chicago, IL). Detailed methods for cell culture and conditioned media are provided in Table S5. HEK293 cells were cultured in DMEM supplemented with 10% fetal bovine serum and 1% penicillin–streptomycin.

Antibodies

The antibodies used were GAPDH and APAF1 from Abcam; anti-p63 4A4 from Neomarkers (for Western blot) and H-129/H137 from Santa Cruz Biotechnology, Inc. (for immunofluorescence); anti-BAK from EMD Millipore; anti–cytochrome *c* from BD; anti–Bcl-XL (H-62), anti–MDM-2 (C-18/N-20), anti-Bcl2 (C-8), and anti-p53 (DO-1) from Santa Cruz Biotechnology, Inc.; anti–phospho-p53 (ser15), anti–phospho-p53 (ser46), anti–Mcl-1, and anti-Puma from Cell Signaling Technology; and anti-Hdmx/MDM4 from Bethyl Laboratories, Inc.

Transfection and DNA-damaging treatments

p63 plasmids were donated by G. Melino (University of Leicester, Leicester, England, UK). HEK293 cells were transfected with Lipofectamine 2000 reagent (Invitrogen) at a 1:2 ml/mg ratio with DNA using 5 mg plasmid DNA. Cells were treated with UV-B as indicated in the figure legends. Cisplatin, etoposide, doxorubicin, dacarbazine, and paclitaxel were used as indicated in the figure legends.

Western blot analysis

Cells were washed in PBS and then lysed using lysis buffer (1 M Tris, 2.5 M NaCl, 10% glycerol, 0.5 M glycerophosphate, 1% Tween 20, 0.5% NP-40, and 1× EDTA-free Complete Protease Inhibitor tablet [Roche]) for 15 min on ice. Extracts were separated on SDS 10 or 12% polyacrylamide gels and transferred to a nitrocellulose transfer membrane (Whatman). The blots were incubated with the specific antibodies and developed according to the manufacturer's instructions (ECL plus; GE Healthcare).

Mitochondrial extracts. This was adapted from published methods (Mihara and Moll, 2003; Arnoult, 2008). Three 10-cm dishes of cells at a confluency of 70–80% were required to obtain sufficient levels of mitochondrial protein. All steps were performed on ice or at 4°C. Each plate was washed once with 1 ml ice-cold PBS/1 mM EDTA before scraping the cells into a 15-ml falcon tube. Cells were pelleted at 750 *g* for 5 min and then washed in 3 ml ice-cold PBS. The cells were pelleted again for 5 min at 750 *g*. The pellet was then resuspended in 400 µl of cold mitochondrial isolation buffer (MIB) with protease inhibitor cocktail (PIC; 1:20). Cells were transferred to an ice-cold Dounce homogenizer (Wheaton) and homogenized with a minimum of 150 strokes, while monitoring under the microscope. Trypan blue staining was used to confirm cell membrane disruption. The solution was transferred to an Eppendorf and centrifuged for 5 min at 800 *g* to isolate the nuclear fraction. The pellet was used for nuclear isolation. The supernatant was centrifuged for 30 min at 10,000 *g* where the resulting pellet contained the mitochondrial fraction. The supernatant containing cytoplasmic proteins was added to the Eppendorf containing the nuclear fraction that was to be used in the nuclear isolation protocol. The mitochondrial pellet was washed in 500 µl of 1× MS buffer (+PIC) and centrifuged again at 10,000 *g* for 15 min. The mitochondrial fraction was resuspended in 50 µl MIB with 1% Triton-X 100. Protein concentration was determined and assayed using SDS-PAGE.

Nuclear and cytoplasmic extracts. The nuclear pellet and cytoplasmic supernatant from the mitochondrial extract method were resuspended and centrifuged at 900 *g* for 5 min at 4°C. The supernatant was discarded. The pellet was resuspended in 300 µl nuclear isolation (NI) lysis buffer supplemented with PIC and incubated on ice for 15 min. This was centrifuged at 3,500 rpm for 10 min at 4°C. The supernatant was transferred to a new Eppendorf-labeled cytoplasmic fraction. The pellet was resuspended again in 300 µl ice-cold NI lysis buffer (+PIC) and centrifuged at 3,500 rpm for 10 min at 4°C, and supernatant was transferred to the cytoplasmic fraction Eppendorf. The nuclear pellet was washed in 1 ml ice-cold Tris-EDTA twice and centrifuged at 3,500 rpm for 10 min at 4°C between each wash. The supernatant was discarded each time. The pellet was resuspended in 300 µl ice-cold TGN lysis buffer (+PIC) and incubated on ice for a total of 30 min, vortexing every 10 min. The sample was centrifuged again at 15,000 rpm for 30 min at 4°C. The protein concentration of the supernatant containing nuclear proteins was determined and assayed using SDS-PAGE.

Immunoprecipitation

Cells were lysed in NP-40 lysis buffer and precleared with protein G beads for 1 h at 4°C. The protein concentration was determined, and then 1 mg of the extract was incubated either with p53 or control IgG antibody prebound to protein G beads for 4 h or overnight at 4°C. The beads were washed twice in NP-40 lysis buffer and twice in 100 mM NaCl, 1 mM EDTA, and 10 mM Tris, pH 8. The immunoprecipitation beads were mixed with 5× Laemmli buffer and loaded onto an SDS–polyacrylamide gel. The gels were transferred (wet) to nitrocellulose membranes, and the resulting blots were incubated with specific antibodies and developed according to the manufacturer's instructions (ECL plus).

RNA isolation, RT, and Q-PCR analysis

RNA was extracted from keratinocytes, fibroblasts, melanocytes, and melanoma cells by using the RNeasy kit (QIAGEN). A total of 500 ng RNA was used for using the SuperScript III RT kit (Invitrogen). The primers used for the PCR were as follows: ΔNp63 forward, 5′-GGAAAACA-ATGCCCAGACTC-3′; and reverse 5′-GAAGGACACGTCGAAAC-TGTG-3′; TAp63 forward, 5′-GGTGCGACAAACAAGATTGAG-3′; and reverse, 5′-GAAGGACACGTCGAAACTGTG-3′; TP53 forward,

5′-GTCACTGCCATGGAGGAGCCGCA-3′; and reverse, 5′-GACGCACACCTATTGCAAGCAAGGGTTC-3′; GAPDH forward, 5′-CTCCTCCACCTTTGACGCTG-3′; and reverse, 5′-CCACCCTGTTGCTGTAGCCA-3′; and GUS forward, 5′-AAACGATTGCAGGGTTTCAC-3′; and reverse, 5′-CTCTCGTCGGTGACTGTTCA-3′.

Q-PCR reactions were set up in 96-well plates using Brilliant II SYBR Green QPCR Master Mix (Agilent Technologies). This Master Mix includes a SureStart Taq DNA polymerase with hot start capability and contains $MgCl_2$ at a concentration of 2.5 mM in the 1× solution. A passive reference dye (ROX) was added to the mix to compensate for non-PCR–related variations in fluorescence. 25-µl reactions were set up. Experimental reactions were performed in triplicate, and duplicate no-template controls were also run. Once sample cDNA was added, the 96-well plate was briefly centrifuged to remove bubbles and ensure mixing. Data were collected by running a three-step cycling protocol using the AB7500 Fast Real-time PCR System (Applied Biosystems). The temperature cycler was set to detect and report fluorescence during the annealing and extension step of each cycle. Formation of nonspecific products was checked using gel analysis. TP63 gene expression levels in samples were standardized to the housekeeping gene, β-glucuronidase (GUS). GUS was chosen because of its stable expression in melanoma cell lines and because it was a medium-expressed gene that was appropriate because of the medium-low expression levels detected for ΔNp63 in RT-PCR experiments. TP63/GUS expression levels in samples were compared with the mean of gene expression levels in the five primary melanocyte cultures to determine the extent of up-regulation of p63 in melanoma cell lines considering a threefold increase in gene expression as a stringent cut-off for significant up-regulation.

Sequencing

RNA was extracted from melanoma cells by using the RNeasy kit, and cDNA was obtained by RT using the SuperScript III RT kit (Invitrogen) according to the manufacturer's instructions. B-RAF (exon 15 for mutations at codon 600) and N-RAS (exons 1–2 for mutations at codons 12, 13, and 61) genes were amplified by PCR with BIOTAQ DNA Polymerase (Bioline) and sequenced with different primers pairs: B-RAF forward, 5′-GCACAGGGCATGGATTACTT-3′; and reverse, 5′-ATTAATCTCTTCATGGCTTT-3′; and N-RAS forward, 5′-CGCCGACTGATTACGTAGC-3′; and reverse, 5′-TCGCCTGTCCTCATGTATTG-3′.

PCR products were sequenced using the BigDye Terminator version 3.1 Cycle Sequencing kit (Applied Biosystems). 0.3 µl PCR product was added to a reaction containing 1 µl BigDye terminator mix (version 3.1; Applied Biosystems), 1 µl of 10 µM primer, and 3 µl Better Buffer (Microzone) made up to 11.5 µl with dH_2O. The following PCR cycle for Sanger sequencing was performed: 95°C for 10 s (25 cycles), followed by 58°C for 15 s (25 cycles) and 60°C for 4 min (25 cycles). Sequencing reactions were transferred to plates and precipitated with 2.5 µl of 125 mM EDTA and 30 µl ice-cold 100% ethanol, left on ice for 10 min, and centrifuged at 4,400 *g* for 20 min. Plates were inverted and centrifuged at 135 *g* for 10 s to remove the supernatant. The pellet was washed with 135 µl of 70% ethanol and centrifuged for 5 min, and the supernatant was removed as before. Samples were dried in a heating block at 95°C for 10 s. Before being loaded on the sequencer, samples were resuspended in 10 µl HiDi formamide, transferred to an ABI plate (both Applied Biosystems), and denatured at 95°C for 3 min. Sequencing reactions were run on a PRISM 3130xl Genetic Analyzer (Applied Biosystems). Samples were viewed and analyzed using Chromas software (Technelysium Pty Ltd).

Gene expression analysis

Total RNA was extracted from 8 primary RGP malignant melanomas, 15 primary vertical growth phase malignant melanomas, and 5 melanoma metastases and processed as described in Scatolini et al. (2010). Commercial RNA (BDTM Human Universal Reference Total RNA; Takara Bio Inc.) was used as baseline in comparative hybridization experiments on oligonucleotide glass arrays (Human Whole Genome 44K Oligo Microarray Array; Agilent Technologies) using a dye-swap duplication scheme. Single channel intensities were then processed and combined with the Resolver SE System (Rosetta Biosoftware). Mean expression intensities and SEs for the *TP63*, *TP53*, and *TP73* genes in the three sample classes were retrieved, as shown in Fig. 1 D.

Fluorescent immunocytochemistry

Cultured cells. Cultured cells were plated onto glass coverslips (confluency of 150,000 cells/cm^2) in 12-well culture plates and allowed to attach overnight at 37°C. Media was discarded and replaced with media containing MitoTracker Orange (dilution 1:10,000). Cells were incubated with MitoTracker Orange for 30–40 min before washing twice in PBS followed by treatment with either UVB or pharmacological drug. Cells were washed in PBS for 5 min at 5–24 h after treatment, fixed in 1 ml of 4% formaldehyde/PBS for 10 min at room temperature, washed twice in fresh PBS for 5 min, and stored at 4°C in PBS. PBS was removed from the cells, and 1 ml of 0.1% Triton X-100 in PBS was added for 3 min at room temperature to allow permeabilization of the cell membranes. Cells were washed twice with PBS for 10 min to remove residual detergent. To avoid nonspecific reaction with the secondary antibody, cells were incubated with 500 µl of 5% goat serum/PBS for 30 min. After removal of the serum, cells were incubated with primary antibody diluted in 5% goat serum/PBS overnight at 4°C. Cells were washed three times for 10 min in PBS and incubated with secondary antibody for 1 h at room temperature in the dark. Cells were washed again three times for 10 min in PBS and incubated with 500 µg/ml DAPI (Invitrogen) for 10 min, followed by two further washes in PBS for 10 min at room temperature. Coverslips were mounted onto a glass slide using Vectashield mounting medium (Vector Laboratories) to prevent photobleaching over time. Mounted slides were sealed with clear colorless nail varnish and stored at 4°C protected from light.

mTMA. Immunohistochemical expression of p63 was investigated in an mTMA (Biomax US ME481) comprising a panel of 8 normal skin cores and 40 melanoma cores, each of 1.5-mm diameter and 5 µM. The slide was initially baked at 60°C for 2 h. Tissue sections were subjected to deparaffinization and rehydration using a xylene and ethanol (EtOH) series: (a) xylene: ×2 at 5 min each, (b) 100% EtOH: twice at 5 min each, (c) 90% EtOH: once at 3 min, (d) 70% EtOH: once at 3 min, (e) 50% EtOH: once at 3 min, (f) distilled water: once at 5 min, and (g) PBS: once at 5 min. The slide was incubated in citrate buffer, pH 6, placed in a microwave at 300 W for 5 min for three cycles, and subsequently cooled for 15 min. It was returned to the microwave for 5 min at 300 W, cooled to room temperature, and incubated in 5% goat serum/PBS for 2 h at room temperature. The slide was placed in a humid chamber and incubated with the primary antibody (1:50 dilution of H137 and H129 anti-p63 antibodies) overnight at 4°C. It was washed in PBS buffer (three times for 10 min) and incubated with the secondary antibodies at room temperature in 5% goat serum/PBS for 1 h. It was washed in PBS (two times for 10 min) followed by 10 min in DAPI in 500 µg/ml PBS and washed (two times for 10 min) in PBS to remove excess DAPI. The slide was mounted using Vectashield to prevent bleaching of fluorophores. HMB-45 was used and is a highly specific marker routinely used in the diagnosis of primary and metastatic melanoma cells to confirm melanoma cells (Colombari et al., 1988; Baisden et al., 2000; Yaziji and Gown, 2003).

RNAi

For p63 knockdown, A375M and WM1158 cell lines were transfected with a SMARTpool of three siRNAs targeting TP63 (ID 217143, ID 4893, and ID 217144; Applied Biosystems). Transfection was performed according to the manufacturer's protocol and optimized for a 6-well plate. Cells were plated at 50% confluency subjected to transfection the following day using HiPerFect (QIAGEN) transfection reagent and 60 nM final concentration of each siRNA. Transfection media was replaced with complete RPMI-1640 media after 24 h. p63 protein expression was analyzed by Western blot at 48 h after transfection. Cells incubated with the transfection reagent only (control) as well as cells transfected with a pool of nontargeting siRNAs (siCONTROL nontargeting siRNA pool) were used as negative controls.

For stable infection with shRNA, the pSUPERIOR.retro.puro vector constructs each containing one of three annealed oligonucleotide sequences targeting p63 (clones 1, 2, and 3) were transfected into the packaging cell line Phoenix cells before introducing the retrovirus into the melanoma cell lines. Infected cells were selected using 0.9–1.25 µg/ml puromycin to establish a stable cell line for shRNA expression that was transcribed in cells from a DNA template as a single-stranded RNA molecule. Effects in p63 mRNA were subsequently analyzed. For p53 knockdown, A375M cells were transfected with the stealth RNAi siRNA for p53 (ID 000546; Invitrogen; Fenouille et al., 2011). Transfection was performed according to the manufacturer's instructions with the Lipofectamine RNAiMAX transfection reagent (Invitrogen).

Flow cytometric analysis of translocation of intracellular proteins

Translocation of p63 and p53 between subcellular compartments was quantified by assessing p63 or p53 fluorescence intensity using a novel flow cytometry technique (Leverrier et al., 2007). The advantages of this method include increased sensitivity, requirement for fewer cells, marginal spillover between cellular compartments, and reproducibility, which allows quantification of relative protein concentration within a cellular compartment. Moreover, data from quantification experiments were validated using confocal microscopy to confirm purity of the fractions (Fig. 3 D). Three different fluorescent stains were used: MitoTracker Orange (CMTMRos; Molecular Probes) for the mitochondria, Hoechst (Bisbenzimide Hoechst 33342; Sigma-Aldrich) for the nucleus, and secondary antibodies conjugated to Cy5 (Cy5-conjugated AffiniPure $F(Ab)_2$ fragment goat anti–mouse IgG; Jackson ImmunoResearch Laboratories, Inc.) for p63 or p53 labeling. Live melanoma cells were incubated with MitoTracker Orange to fluorescently label mitochondria, and cells were labeled with anti-p63 or IgG mouse isotype primary antibody and Cy5-conjugated anti–mouse secondary antibody followed by Hoechst (to label the nuclei). The anti-p63 antibody used (4A4) detected all isoforms of p63. Intact A375M cells, characterized by their double positivity to Hoechst and MitoTracker Orange labeling, were analyzed. Cells were disrupted using a Dounce homogenizer, and the resulting homogenates were reanalyzed by flow cytometry. For each cell line, preliminary control experiments included MitoTracker Orange or Hoechst fluorescently labeled cells only, confirming location of the fractions in the homogenized sample. Hoechst-positive and MitoTracker Orange–negative populations were defined as free nuclei; Hoechst-negative and MitoTracker–positive populations were defined as free mitochondria ,and the final region gated comprised intact cells. After gating for whole cell, mitochondrial, and nuclear populations, fluorescence intensity of p63-Cy5 was analyzed using the FlowJo software (Tree Star). To establish purity of the nuclear and mitochondrial fractions, homogenized cells were sorted according to Hoechst and MitoTracker Orange labeling using the FACSAria cell sorter (BD). Sorted fractions were reanalyzed to confirm purity of each fraction (Fig. 3 D). Sorted mitochondrial fractions were centrifuged (13,000 *g* for 30 min at 4°C), and the supernatant was discarded. Mitochondrial isolates fluorescently labeled with MitoTracker Orange were mounted and visualized using confocal microscopy. The nuclear fraction was prepared in the same way except centrifugation was performed at 4,500 rpm for 15 min at 4°C before mounting isolates onto a slide. Imaging of the intact cells, nuclei, and mitochondria by confocal microscopy validated the analysis gates used to separate fractions comprising of pure nuclei and mitochondria and not fragments of cells. Further verification of this technique included detection of p63 protein by visualizing p63-Cy5 in mitochondrial and nuclear fractions using confocal microscopy after fluorescence-activated cell sorting (FACSAria flow cytometer; BD; Fig. 3 E). An LSRII (BD) fitted with 488-, 405-, 350–360-, and 633-nm lasers with FACS Diva software version 4.1.2 was used to acquire 30,000 whole cells or 1 million fractionated events, using the Argon 488-nm laser line and a 575/26-nm band pass filter to detect MitoTracker Orange; the UV 350–360 laser and a 440/40-nm band pass filter were used to detect Hoechst 33342; the Red HeNe 633-nm line and 660/20-nm band pass filter were used to detect Cy5. No compensation was required because of the use of separate laser lines to detect fluorophores, which did not display any spectral cross talk.

Flow cytometric analysis of apoptosis

The Annexin V assay was used to detect apoptotic cells. Cells were treated with chemotherapeutic agents for 16–24 h, with or without prior DNA transfection or shRNA infection. Cells were trypsinized, and all cells (living and dead) were pelleted. Cells were resuspended in 400 µl of 1× Binding Buffer (BD; 10× binding buffer, 0.1 M Hepes, pH 7.4, 1.4 M NaCl, and 25 mM $CaCl_2$). 5 µl Annexin V–FITC (BD) was added and incubated in the dark at room temperature for 15 min. Samples were analyzed on the flow cytometer (LSRII) within an hour. Viability dye (5 µg/ml propidium iodide [PI]) was added just before reading. The following controls were used to set up compensation and quadrants: unstained cells, cells stained with Annexin V–FITC only (no PI), and cells stained with PI only (no Annexin V–FITC). Apoptotic cell populations included Annexin V–FITC positive, PI negative and Annexin V–FITC positive, and PI positive (right top and bottom quadrants of scatter plot). Results were analyzed using the FACSDiva software (BD) and expressed as mean ± SEM values of three independent experiments performed in triplicate.

Electron microscopy

The Tokuyasu method was used for immunogold localization of p63 (Tokuyasu, 1980). Cells were seeded at 70% confluency in two 100-mm plates and treated with 2 µM paclitaxel for 6 h. 8% formaldehyde + 0.2% glutaraldehyde in 100 mM Pipes buffer, pH 7.2, was added to the media (1:1), and plates were refrigerated (1 h). Cells were scraped into an Eppendorf tube and centrifuged (1,500 rpm for 5 min). The supernatant was discarded, and cells were resuspended in Pipes buffer for transport. The pellet was washed twice in Pipes buffer, and supernatant was discarded, ensuring removal of fixative. The pellet was resuspended in 10% warm gelatin and centrifuged (6,000 rpm for 5 min). To solidify, the pellet of cells in gelatin was incubated at 4°C (30 min). Gelatin containing the cells was cut into small cubes ~1 mm^3, which were incubated in 2.3 M sucrose at 4°C overnight for cryoprotection. Cubes were mounted on specimen pins, excess sucrose was blotted away, and the cubes were cryofixed by plunging into liquid nitrogen. Cryosections, 90-nm thick, were cut from these blocks with glass knives at −100°C using an MTXL ultra-microtome with a CRX cryo-adaptation (RMC). Groups of sections were picked up on a droplet of 2.3 M sucrose and transferred onto Pioloform-coated nickel grids. Grids were floated onto standard buffer consisting of PBS + 1% BSA + 0.1% sodium azide, pH 7.4. Grids were incubated (three times for 5 min) on PBS–0.05 M glycine to remove remaining aldehyde groups persisting from the fixation process before being washed in incubation buffer (PBS + 0.1% BSA-c [Aurion] + 0.1% azide, pH 7.4) and transferred onto droplets of primary antibody (anti-p63 antibodies H129, 4A4, and H137 [Santa Cruz Biotechnology, Inc.] and anti-mtHsp70 [Grp75; Abcam]) diluted in incubation buffer (1:50) for overnight incubation at 4°C. The primary antibody was removed by passing over six droplets of incubation buffer solution, 5 min per droplet, before incubation for 1 h at room temperature with the secondary antibody, diluted in incubation buffer (1:100). Secondary antibody was removed by passing grids over three droplets of PBS (5 min), and the reaction was fixed by exposing grids to PBS–2% glutaraldehyde. Grids were washed over distilled water (three times for 5 min). Sections were subsequently embedded in 2% methylcellulose/3% uranyl acetate solution in a 9:1 ratio. Sections were examined, and micrographs were obtained using a T12 transmission electron microscope (FEI) at an accelerating voltage of 120 kV.

Immunohistochemistry: paraffin-embedded tissue

Clinicopathologically characterized, formalin-fixed paraffin-embedded material representing benign melanocytic nevi and all stages of melanoma development (primary melanoma, recurrent melanoma, and metastases) were analyzed for expression of p63 (Ethical approval number 07/QO604/23 by the East London & The City HA Local Research Ethics committee 2, UK). The effect of storage of tissue samples on p63 reactivity was notable; with increased storage times, a progressive and significant decrease in intensity of p63 staining was observed, with evidence of significant decline occurring as early as 2 wk of storage (Hameed and Humphrey, 2005; Burford et al., 2009).

We also observed this effect and therefore, for optimal detection of p63 in tissue samples, staining was undertaken within 2 wk of sectioning of tumor samples.

Melanoma tissue samples representing different stages of disease progression were selected from the archive of paraffin-embedded tissue samples at Barts and the London National Health Service Trust. Clinical data were collected from patients attending the skin cancer multidisciplinary clinic and through accessing electronic medical records. Pathology reports confirmed the diagnosis of melanoma in all cases, and slides were subsequently reviewed by a dermatopathologist (R. Cerio). Immunostaining was undertaken with a Vector RTU system (red). Initial optimization was performed using anti-p63 antibodies H129 and 4A4 (dilution 1:100). Vector VIP (SIC-4600) was applied for 20 min, and a green counterstain was used to distinguish the red stain clearly. As both anti-p63 antibodies demonstrated similar p63 reactivity, the H129 antibody (routinely used for the analysis of clinical samples and for clinical trials by the Barts Pathology Service) was used for all tumor samples.

Positive reactivity to p63 in basal keratinocytes in the epidermis or ductal/glandular epithelia in the dermis of skin samples was used as a positive internal control. Negative controls comprised omission of the primary antibody. Positive reactivity of p63 in melanoma tumor samples was confirmed when melanoma cells showed staining of nucleus and/or cytoplasm. Nevi and melanoma sections labeled with p63 were reviewed by three dermatologists (R.N. Matin, C.A. Harwood, and S. Law Pak Chong) and one dermatopathologist (R. Cerio) blinded to clinical outcomes. Given the heterogeneity displayed by melanoma cells, only tumors demonstrating >50% positive reactivity of melanoma cells were included in the statistical analysis.

Statistical analysis

Statistical analysis was undertaken in collaboration with D. Mesher (Centre for Cancer Prevention, QMUL). Clinicopathological variables were tabulated and compared with p63 status. A power calculation was performed using melanoma-specific death as the primary end point. For 80% power, 200 melanomas from individuals with follow up over 5 yr needed to be analyzed to detect a 5% significant difference in outcomes between p63-positive and -negative tumors. For survival (overall and melanoma-specific analysis), patients were censored at date of death or date of last follow up. For recurrence and metastases, patients were censored at date of recurrence/metastases, date of death, or date of last follow up. Analysis of end points was performed by Cox proportional hazards model. Where non-independent observations were included in Cox regression analysis (i.e., multiple tumors from the same patient), robust SEs were used to adjust for this using the cluster option in Stata. Variables were examined univariately, and subsequently a multivariate model was constructed using backward stepwise selection method. P-values were presented comparing the multivariate model with and without p63 status included. All p-values were two-sided, and all statistical analyses were performed using Stata 10.0.

Online supplemental material

Table S1 provides statistical analysis of demographic data for p63-expressing primary melanoma tissue samples (mTMA). Tables S2 and S3 show the clinicopathological features of primary and metastatic melanoma archival tissue samples, respectively. Table S4 summarizes the mutational status of p53, BRAF, and NRAS in melanoma cell lines used in the study. Table S5 shows the culture media and supplements for the melanocytes and established melanoma cell lines used in the study. Online supplemental material is available at http://www.jem.org/cgi/content/full/jem.20121439/DC1.

We are grateful to Dr. Gary Warnes, Flow Cytometry Core Facility Manager, for technical advice, to Dr. Claire Scott for the BRAF and NRAS mutation sequencing of the cell lines, and to the core Pathology laboratory for the technical support with the tissue sample immunostaining at the Blizard Institute. We also thank Dr. Alice Warley (Centre for Ultrastructural Imaging CUI at King's College London, London, England, UK) for technical advice with transmission electron microscopy methods.

Funding support was provided by the Medical Research Council, Cancer Research UK, and Barts and The London Charity.

The authors declare no competing financial interests.

Submitted: 3 July 2012
Accepted: 18 January 2013

REFERENCES

Akslen, L.A., and O. Mørkve. 1992. Expression of p53 protein in cutaneous melanoma. *Int. J. Cancer.* 52:13–16. http://dx.doi.org/10.1002/ijc.2910520104

Albino, A.P., M.J. Vidal, N.S. McNutt, C.R. Shea, V.G. Prieto, D.M. Nanus, J.M. Palmer, and N.K. Hayward. 1994. Mutation and expression of the p53 gene in human malignant melanoma. *Melanoma Res.* 4:35–45. http://dx.doi.org/10.1097/00008390-199402000-00006

Arima, Y., M. Nitta, S. Kuninaka, D. Zhang, T. Fujiwara, Y. Taya, M. Nakao, and H. Saya. 2005. Transcriptional blockade induces p53-dependent apoptosis associated with translocation of p53 to mitochondria. *J. Biol. Chem.* 280:19166–19176. http://dx.doi.org/10.1074/jbc.M410691200

Arnoult, D. 2008. Apoptosis-associated mitochondrial outer membrane permeabilization assays. *Methods.* 44:229–234. http://dx.doi.org/10.1016/j.ymeth.2007.11.003

Avery-Kiejda, K.A., X.D. Zhang, L.J. Adams, R.J. Scott, B. Vojtesek, D.P. Lane, and P. Hersey. 2008. Small molecular weight variants of p53 are expressed in human melanoma cells and are induced by the DNA-damaging agent cisplatin. *Clin. Cancer Res.* 14:1659–1668. http://dx.doi.org/10.1158/1078-0432.CCR-07-1422

Avery-Kiejda, K.A., N.A. Bowden, A.J. Croft, L.L. Scurr, C.F. Kairupan, K.A. Ashton, B.A. Talseth-Palmer, H. Rizos, X.D. Zhang, R.J. Scott, and P. Hersey. 2011. P53 in human melanoma fails to regulate target genes associated with apoptosis and the cell cycle and may contribute to proliferation. *BMC Cancer.* 11:203. http://dx.doi.org/10.1186/1471-2407-11-203

Azzola, M.F., H.M. Shaw, J.F. Thompson, S.J. Soong, R.A. Scolyer, G.F. Watson, M.H. Colman, and Y. Zhang. 2003. Tumor mitotic rate is a more powerful prognostic indicator than ulceration in patients with primary cutaneous melanoma: an analysis of 3661 patients from a single center. *Cancer.* 97:1488–1498. http://dx.doi.org/10.1002/cncr.11196

Bae, I., M.L. Smith, M.S. Sheikh, Q. Zhan, D.A. Scudiero, S.H. Friend, P.M. O'Connor, and A.J. Fornace Jr. 1996. An abnormality in the p53 pathway following gamma-irradiation in many wild-type p53 human melanoma lines. *Cancer Res.* 56:840–847.

Baisden, B.L., F.B. Askin, J.R. Lange, and W.H. Westra. 2000. HMB-45 immunohistochemical staining of sentinel lymph nodes: a specific method for enhancing detection of micrometastases in patients with melanoma. *Am. J. Surg. Pathol.* 24:1140–1146. http://dx.doi.org/10.1097/00000478-200008000-00012

Bardeesy, N., K.K. Wong, R.A. DePinho, and L. Chin. 2000. Animal models of melanoma: recent advances and future prospects. *Adv. Cancer Res.* 79:123–156. http://dx.doi.org/10.1016/S0065-230X(00)79004-X

Bártek, J., J. Bártková, B. Vojtěsek, Z. Stasková, J. Lukás, A. Rejthar, J. Kovarík, C.A. Midgley, J.V. Gannon, and D.P. Lane. 1991. Aberrant expression of the p53 oncoprotein is a common feature of a wide spectrum of human malignancies. *Oncogene.* 6:1699–1703.

Belmar-Lopez, C., P. Mancheno-Corvo, M.A. Saornil, P. Baril, G. Vassaux, M. Quintanilla, and P. Martin-Duque. 2008. Uveal vs. cutaneous melanoma. Origins and causes of the differences. *Clin. Transl. Oncol.* 10:137–142. http://dx.doi.org/10.1007/s12094-008-0170-4

Benchimol, S. 2004. p53—an examination of sibling support in apoptosis control. *Cancer Cell.* 6:3–4. http://dx.doi.org/10.1016/j.ccr.2004.07.002

Bourne, T.D., A.M. Bellizzi, E.B. Stelow, A.H. Loy, P.A. Levine, M.R. Wick, and S.E. Mills. 2008. p63 Expression in olfactory neuroblastoma and other small cell tumors of the sinonasal tract. *Am. J. Clin. Pathol.* 130:213–218. http://dx.doi.org/10.1309/TEDD2FCWH8W0H4HA

Brinck, U., I. Ruschenburg, C.J. Di Como, N. Buschmann, H. Betke, J. Stachura, C. Cordon-Cardo, and M. Korabiowska. 2002. Comparative study of p63 and p53 expression in tissue microarrays of malignant melanomas. *Int. J. Mol. Med.* 10:707–711.

Burford, H.N., A.L. Adams, and O. Hameed. 2009. Effect of storage on p63 immunohistochemistry: a time-course study. *Appl. Immunohistochem. Mol. Morphol.* 17:68–71. http://dx.doi.org/10.1097/PAI.0b013e31818110de

Chan, I., J.I. Harper, J.E. Mellerio, and J.A. McGrath. 2004. ADULT ectodermal dysplasia syndrome resulting from the missense mutation R298Q in the p63 gene. *Clin. Exp. Dermatol.* 29:669–672. http://dx.doi.org/10.1111/j.1365-2230.2004.01643.x

Chehab, N.H., A. Malikzay, M. Appel, and T.D. Halazonetis. 2000. Chk2/hCds1 functions as a DNA damage checkpoint in G(1) by stabilizing p53. *Genes Dev.* 14:278–288.

Chipuk, J.E., U. Maurer, D.R. Green, and M. Schuler. 2003. Pharmacologic activation of p53 elicits Bax-dependent apoptosis in the absence of transcription. *Cancer Cell.* 4:371–381. http://dx.doi.org/10.1016/S1535-6108(03)00272-1

Chipuk, J.E., L. Bouchier-Hayes, T. Kuwana, D.D. Newmeyer, and D.R. Green. 2005. PUMA couples the nuclear and cytoplasmic proapoptotic function of p53. *Science.* 309:1732–1735. http://dx.doi.org/10.1126/science.1114297

Choi, H.R., J.G. Batsakis, F. Zhan, E. Sturgis, M.A. Luna, and A.K. El-Naggar. 2002. Differential expression of p53 gene family members p63 and p73 in head and neck squamous tumorigenesis. *Hum. Pathol.* 33:158–164. http://dx.doi.org/10.1053/hupa.2002.30722

Colombari, R., F. Bonetti, G. Zamboni, A. Scarpa, F. Marino, A. Tomezzoli, P. Capelli, F. Menestrina, M. Chilosi, and L. Fiore-Donati. 1988. Distribution of melanoma specific antibody (HMB-45) in benign and malignant melanocytic tumours. An immunohistochemical study on paraffin sections. *Virchows Arch. A Pathol. Anat. Histopathol.* 413:17–24. http://dx.doi.org/10.1007/BF00844277

Dellavalle, R.P., T.B. Egbert, A. Marchbank, L.J. Su, L.A. Lee, and P. Walsh. 2001. CUSP/p63 expression in rat and human tissues. *J. Dermatol. Sci.* 27:82–87. http://dx.doi.org/10.1016/S0923-1811(01)00105-0

Dhillon, P.K., M. Barry, M.J. Stampfer, S. Perner, M. Fiorentino, A. Fornari, J. Ma, J. Fleet, T. Kurth, M.A. Rubin, and L.A. Mucci. 2009. Aberrant cytoplasmic expression of p63 and prostate cancer mortality. *Cancer Epidemiol. Biomarkers Prev.* 18:595–600. http://dx.doi.org/10.1158/1055-9965.EPI-08-0785

Di Como, C.J., M.J. Urist, I. Babayan, M. Drobnjak, C.V. Hedvat, J. Teruya-Feldstein, K. Pohar, A. Hoos, and C. Cordon-Cardo. 2002. p63 expression profiles in human normal and tumor tissues. *Clin. Cancer Res.* 8:494–501.

Dotto, J.E., and E.J. Glusac. 2006. p63 is a useful marker for cutaneous spindle cell squamous cell carcinoma. *J. Cutan. Pathol.* 33:413–417. http://dx.doi.org/10.1111/j.0303-6987.2006.00477.x

el-Deiry, W.S., T. Tokino, T. Waldman, J.D. Oliner, V.E. Velculescu, M. Burrell, D.E. Hill, E. Healy, J.L. Rees, S.R. Hamilton, et al. 1995. Topological control of p21WAF1/CIP1 expression in normal and neoplastic tissues. *Cancer Res.* 55:2910–2919.

Fenouille, N., A. Puissant, M. Tichet, G. Zimniak, P. Abbe, A. Mallavialle, S. Rocchi, J.P. Ortonne, M. Deckert, R. Ballotti, and S. Tartare-Deckert. 2011. SPARC functions as an anti-stress factor by inactivating p53 through Akt-mediated MDM2 phosphorylation to promote melanoma cell survival. *Oncogene.* 30:4887–4900. http://dx.doi.org/10.1038/onc.2011.198

Flores, E.R., K.Y. Tsai, D. Crowley, S. Sengupta, A. Yang, F. McKeon, and T. Jacks. 2002. p63 and p73 are required for p53-dependent apoptosis in response to DNA damage. *Nature.* 416:560–564. http://dx.doi.org/10.1038/416560a

Flores, E.R., S. Sengupta, J.B. Miller, J.J. Newman, R. Bronson, D. Crowley, A. Yang, F. McKeon, and T. Jacks. 2005. Tumor predisposition in mice mutant for p63 and p73: evidence for broader tumor suppressor functions for the p53 family. *Cancer Cell.* 7:363–373. http://dx.doi.org/10.1016/j.ccr.2005.02.019

Fukushima, N., T. Satoh, N. Sueoka, A. Sato, M. Ide, T. Hisatomi, N. Kuwahara, R. Tomimasu, N. Tsuneyoshi, N. Funai, et al. 2006. Clinicopathological characteristics of p63 expression in B-cell lymphoma. *Cancer Sci.* 97:1050–1055. http://dx.doi.org/10.1111/j.1349-7006.2006.00284.x

Gembarska, A., F. Luciani, C. Fedele, E.A. Russell, M. Dewaele, S. Villar, A. Zwolinska, S. Haupt, J. de Lange, D. Yip, et al. 2012. MDM4 is a key therapeutic target in cutaneous melanoma. *Nat. Med.* 18:1239–1247. http://dx.doi.org/10.1038/nm.2863

Glusac, E.J. 2011. The melanoma 'epidemic', a dermatopathologist's perspective. *J. Cutan. Pathol.* 38:264–267. http://dx.doi.org/10.1111/j.1600-0560.2010.01660.x

Gomez-Monterrey, I., A. Bertamino, A. Porta, A. Carotenuto, S. Musella, C. Aquino, I. Granata, M. Sala, D. Brancaccio, D. Picone, et al. 2010. Identification of the Spiro(oxindole-3,3′-thiazolidine)-Based Derivatives as Potential p53 Activity Modulators. *J. Med. Chem.* 53:8319–8329. http://dx.doi.org/10.1021/jm100838z

Gressner, O., T. Schilling, K. Lorenz, E. Schulze Schleithoff, A. Koch, H. Schulze-Bergkamen, A.M. Lena, E. Candi, A. Terrinoni, M.V. Catani, et al. 2005. TAp63alpha induces apoptosis by activating signaling via death receptors and mitochondria. *EMBO J.* 24:2458–2471. http://dx.doi.org/10.1038/sj.emboj.7600708

Hameed, O., and P.A. Humphrey. 2005. p63/AMACR antibody cocktail restaining of prostate needle biopsy tissues after transfer to charged slides: a viable approach in the diagnosis of small atypical foci that are lost on block sectioning. *Am. J. Clin. Pathol.* 124:708–715. http://dx.doi.org/10.1309/JXK1BVATGBVNQ9J9

Harmes, D.C., E. Bresnick, E.A. Lubin, J.K. Watson, K.E. Heim, J.C. Curtin, A.M. Suskind, J. Lamb, and J. DiRenzo. 2003. Positive and negative regulation of deltaN-p63 promoter activity by p53 and deltaN-p63-alpha contributes to differential regulation of p53 target genes. *Oncogene.* 22:7607–7616. http://dx.doi.org/10.1038/sj.onc.1207129

Hibi, K., B. Trink, M. Patturajan, W.H. Westra, O.L. Caballero, D.E. Hill, E.A. Ratovitski, J. Jen, and D. Sidransky. 2000. AIS is an oncogene amplified in squamous cell carcinoma. *Proc. Natl. Acad. Sci. USA.* 97:5462–5467. http://dx.doi.org/10.1073/pnas.97.10.5462

Hirao, A., Y.Y. Kong, S. Matsuoka, A. Wakeham, J. Ruland, H. Yoshida, D. Liu, S.J. Elledge, and T.W. Mak. 2000. DNA damage-induced activation of p53 by the checkpoint kinase Chk2. *Science.* 287:1824–1827. http://dx.doi.org/10.1126/science.287.5459.1824

Hocker, T., and H. Tsao. 2007. Ultraviolet radiation and melanoma: a systematic review and analysis of reported sequence variants. *Hum. Mutat.* 28:578–588. http://dx.doi.org/10.1002/humu.20481

Hoek, K., D.L. Rimm, K.R. Williams, H. Zhao, S. Ariyan, A. Lin, H.M. Kluger, A.J. Berger, E. Cheng, E.S. Trombetta, et al. 2004. Expression profiling reveals novel pathways in the transformation of melanocytes to melanomas. *Cancer Res.* 64:5270–5282. http://dx.doi.org/10.1158/0008-5472.CAN-04-0731

Houben, R., S. Hesbacher, C.P. Schmid, C.S. Kauczok, U. Flohr, S. Haferkamp, C.S. Müller, D. Schrama, J. Wischhusen, and J.C. Becker. 2011. High-level expression of wild-type p53 in melanoma cells is frequently associated with inactivity in p53 reporter gene assays. *PLoS ONE.* 6:e22096. http://dx.doi.org/10.1371/journal.pone.0022096

Hu, H., S.H. Xia, A.D. Li, X. Xu, Y. Cai, Y.L. Han, F. Wei, B.S. Chen, X.P. Huang, Y.S. Han, et al. 2002. Elevated expression of p63 protein in human esophageal squamous cell carcinomas. *Int. J. Cancer.* 102:580–583. http://dx.doi.org/10.1002/ijc.10739

Hussein, M.R., A.K. Haemel, and G.S. Wood. 2003. p53-related pathways and the molecular pathogenesis of melanoma. *Eur. J. Cancer Prev.* 12:93–100. http://dx.doi.org/10.1097/00008469-200304000-00002

Ikawa, S., A. Nakagawara, and Y. Ikawa. 1999. p53 family genes: structural comparison, expression and mutation. *Cell Death Differ.* 6:1154–1161. http://dx.doi.org/10.1038/sj.cdd.4400631

Jacobs, W.B., G. Govoni, D. Ho, J.K. Atwal, F. Barnabe-Heider, W.M. Keyes, A.A. Mills, F.D. Miller, and D.R. Kaplan. 2005. p63 is an essential proapoptotic protein during neural development. *Neuron.* 48:743–756. http://dx.doi.org/10.1016/j.neuron.2005.10.027

Ji, Z., C.N. Njauw, M. Taylor, V. Neel, K.T. Flaherty, and H. Tsao. 2012. p53 rescue through HDM2 antagonism suppresses melanoma growth and potentiates MEK inhibition. *J. Invest. Dermatol.* 132:356–364. http://dx.doi.org/10.1038/jid.2011.313

Kakudo,Y., H. Shibata, K. Otsuka, S. Kato, and C. Ishioka. 2005. Lack of correlation between p53-dependent transcriptional activity and the ability to induce apoptosis among 179 mutant p53s. *Cancer Res.* 65:2108–2114. http://dx.doi.org/10.1158/0008-5472.CAN-04-2935

Kanner, W.A., L.B. Brill II, J.W. Patterson, and M.R. Wick. 2010. CD10, p63 and CD99 expression in the differential diagnosis of atypical fibroxanthoma, spindle cell squamous cell carcinoma and desmoplastic melanoma. *J. Cutan. Pathol.* 37:744–750. http://dx.doi.org/10.1111/j.1600-0560.2010.01534.x

Kanoko, M., M. Ueda, T. Nagano, and M. Ichihashi. 1996. Expression of p53 protein in melanoma progression. *J. Dermatol. Sci.* 12:97–103. http://dx.doi.org/10.1016/0923-1811(95)00465-3

Karst, A.M., D.L. Dai, M. Martinka, and G. Li. 2005. PUMA expression is significantly reduced in human cutaneous melanomas. *Oncogene.* 24: 1111–1116. http://dx.doi.org/10.1038/sj.onc.1208374

Katoh, I., K.I. Aisaki, S.I. Kurata, S. Ikawa, and Y. Ikawa. 2000. p51A (TAp63gamma), a p53 homolog, accumulates in response to DNA damage for cell regulation. *Oncogene.* 19:3126–3130. http://dx.doi.org/10.1038/sj.onc.1203644

Keyes, W.M., Y. Wu, H. Vogel, X. Guo, S.W. Lowe, and A.A. Mills. 2005. p63 deficiency activates a program of cellular senescence and leads to accelerated aging. *Genes Dev.* 19:1986–1999. http://dx.doi.org/10.1101/gad.342305

Kilic, E., H.T. Brüggenwirth, M. Meier, N.C. Naus, H.B. Beverloo, J.P. Meijerink, G.P. Luyten, and A. de Klein. 2008. Increased expression of p73Deltaex2 transcript in uveal melanoma with loss of chromosome 1p. *Melanoma Res.* 18:208–213. http://dx.doi.org/10.1097/CMR.0b013e3283036aa1

Knopf, A., C. Plettenberg, A. Pickhard, M. Bas, J. Reifenberger, H. Bier, and V. Balz. 2011. Analysis of the functional integrity of the p53 tumor-suppressor gene in malignant melanoma. *Melanoma Res.* 21:380–388. http://dx.doi.org/10.1097/CMR.0b013e328347ee04

Koga, F., S. Kawakami, Y. Fujii, K. Saito, Y. Ohtsuka, A. Iwai, N. Ando, T. Takizawa, Y. Kageyama, and K. Kihara. 2003. Impaired p63 expression associates with poor prognosis and uroplakin III expression in invasive urothelial carcinoma of the bladder. *Clin. Cancer Res.* 9:5501–5507.

Koster, M.I., S. Kim, J. Huang, T. Williams, and D.R. Roop. 2006. TAp63alpha induces AP-2gamma as an early event in epidermal morphogenesis. *Dev. Biol.* 289:253–261. http://dx.doi.org/10.1016/j.ydbio.2005.10.041

Kulesz-Martin, M., J. Lagowski, S. Fei, C. Pelz, R. Sears, M.B. Powell, R. Halaban, and J. Johnson. 2005. Melanocyte and keratinocyte carcinogenesis: p53 family protein activities and intersecting mRNA expression profiles. *J. Investig. Dermatol. Symp. Proc.* 10:142–152. http://dx.doi.org/10.1111/j.1087-0024.2005.200405.x

Lassam, N.J., L. From, and H.J. Kahn. 1993. Overexpression of p53 is a late event in the development of malignant melanoma. *Cancer Res.* 53:2235–2238.

Leverrier, S., D. Bergamaschi, L. Ghali, A. Ola, G. Warnes, B. Akgül, K. Blight, R. García-Escudero, A. Penna, A. Eddaoudi, and A. Storey. 2007. Role of HPV E6 proteins in preventing UVB-induced release of pro-apoptotic factors from the mitochondria. *Apoptosis.* 12:549–560. http://dx.doi.org/10.1007/s10495-006-0004-1

Li, B., Q. Cheng, Z. Li, and J. Chen. 2010. p53 inactivation by MDM2 and MDMX negative feedback loops in testicular germ cell tumors. *Cell Cycle.* 9:1411–1420.

Liefer, K.M., M.I. Koster, X.J. Wang, A. Yang, F. McKeon, and D.R. Roop. 2000. Down-regulation of p63 is required for epidermal UV-B-induced apoptosis. *Cancer Res.* 60:4016–4020.

Little, N.A., and A.G. Jochemsen. 2001. Hdmx and Mdm2 can repress transcription activation by p53 but not by p63. *Oncogene.* 20:4576–4580. http://dx.doi.org/10.1038/sj.onc.1204615

MacPartlin, M., S. Zeng, H. Lee, D. Stauffer, Y. Jin, M. Thayer, and H. Lu. 2005. p300 regulates p63 transcriptional activity. *J. Biol. Chem.* 280: 30604–30610. http://dx.doi.org/10.1074/jbc.M503352200

Mancini, F., G. Di Conza, M. Pellegrino, C. Rinaldo, A. Prodosmo, S. Giglio, I. D'Agnano, F. Florenzano, L. Felicioni, F. Buttitta, et al. 2009. MDM4 (MDMX) localizes at the mitochondria and facilitates the p53-mediated intrinsic-apoptotic pathway. *EMBO J.* 28:1926–1939. http://dx.doi.org/10.1038/emboj.2009.154

Mangiulli, M., A. Valletti, M.F. Caratozzolo, A. Tullo, E. Sbisà, G. Pesole, and A.M. D'Erchia. 2009. Identification and functional characterization of two new transcriptional variants of the human p63 gene. *Nucleic Acids Res.* 37:6092–6104. http://dx.doi.org/10.1093/nar/gkp674

Marchenko, N.D., S. Wolff, S. Erster, K. Becker, and U.M. Moll. 2007. Monoubiquitylation promotes mitochondrial p53 translocation. *EMBO J.* 26:923–934. http://dx.doi.org/10.1038/sj.emboj.7601560

Marchini, S., M. Marabese, E. Marrazzo, P. Mariani, D. Cattaneo, R. Fossati, A. Compagnoni, R. Fruscio, A.A. Lissoni, and M. Broggini. 2008. DeltaNp63 expression is associated with poor survival in ovarian cancer. *Ann. Oncol.* 19:501–507. http://dx.doi.org/10.1093/annonc/mdm519

Massion, P.P., P.M. Taflan, S.M. Jamshedur Rahman, P. Yildiz, Y. Shyr, M.E. Edgerton, M.D. Westfall, J.R. Roberts, J.A. Pietenpol, D.P. Carbone, and A.L. Gonzalez. 2003. Significance of p63 amplification and overexpression in lung cancer development and prognosis. *Cancer Res.* 63:7113–7121.

Matsuoka, S., M. Huang, and S.J. Elledge. 1998. Linkage of ATM to cell cycle regulation by the Chk2 protein kinase. *Science.* 282:1893–1897. http://dx.doi.org/10.1126/science.282.5395.1893

McGregor, J.M., C.C. Yu, E.A. Dublin, D.M. Barnes, D.A. Levison, and D.M. MacDonald. 1993. p53 immunoreactivity in human malignant melanoma and dysplastic naevi. *Br. J. Dermatol.* 128:606–611. http://dx.doi.org/10.1111/j.1365-2133.1993.tb00253.x

Merlino, G., and F.P. Noonan. 2003. Modeling gene-environment interactions in malignant melanoma. *Trends Mol. Med.* 9:102–108. http://dx.doi.org/10.1016/S1471-4914(03)00006-6

Michaelis, M., F. Rothweiler, S. Barth, J. Cinatl, M. van Rikxoort, N. Löschmann, Y. Voges, R. Breitling, A. von Deimling, F. Rödel, et al. 2011. Adaptation of cancer cells from different entities to the MDM2 inhibitor nutlin-3 results in the emergence of p53-mutated multi-drug-resistant cancer cells. *Cell Death Dis.* 2:e243. http://dx.doi.org/10.1038/cddis.2011.129

Mihara, M., and U.M. Moll. 2003. Detection of mitochondrial localization of p53. *Methods Mol. Biol.* 234:203–209.

Mills, A.A. 2006. p63: oncogene or tumor suppressor? *Curr. Opin. Genet. Dev.* 16:38–44. http://dx.doi.org/10.1016/j.gde.2005.12.001

Moll, U.M., N. Marchenko, and X.K. Zhang. 2006. p53 and Nur77/TR3 - transcription factors that directly target mitochondria for cell death induction. *Oncogene.* 25:4725–4743. http://dx.doi.org/10.1038/sj.onc.1209601

Morgan, M.B., C. Purohit, and T.R. Anglin. 2008. Immunohistochemical distinction of cutaneous spindle cell carcinoma. *Am. J. Dermatopathol.* 30:228–232. http://dx.doi.org/10.1097/DAD.0b013e31816de820

Müller, M., E.S. Schleithoff, W. Stremmel, G. Melino, P.H. Krammer, and T. Schilling. 2006. One, two, three—p53, p63, p73 and chemosensitivity. *Drug Resist. Updat.* 9:288–306. http://dx.doi.org/10.1016/j.drup.2007.01.001

Mundt, H.M., W. Stremmel, G. Melino, P.H. Krammer, T. Schilling, and M. Müller. 2010. Dominant negative (DeltaN) p63alpha induces drug resistance in hepatocellular carcinoma by interference with apoptosis signaling pathways. *Biochem. Biophys. Res. Commun.* 396:335–341. http://dx.doi.org/10.1016/j.bbrc.2010.04.093

Muthusamy, V., C. Hobbs, C. Nogueira, C. Cordon-Cardo, P.H. McKee, L. Chin, and M.W. Bosenberg. 2006. Amplification of CDK4 and MDM2 in malignant melanoma. *Genes Chromosomes Cancer.* 45:447–454. http://dx.doi.org/10.1002/gcc.20310

Narahashi, T., T. Niki, T. Wang, A. Goto, D. Matsubara, N. Funata, and M. Fukayama. 2006. Cytoplasmic localization of p63 is associated with poor patient survival in lung adenocarcinoma. *Histopathology.* 49:349–357. http://dx.doi.org/10.1111/j.1365-2559.2006.02507.x

Nemajerova, A., S. Erster, and U.M. Moll. 2005. The post-translational phosphorylation and acetylation modification profile is not the determining factor in targeting endogenous stress-induced p53 to mitochondria. *Cell Death Differ.* 12:197–200. http://dx.doi.org/10.1038/sj.cdd.4401526

Oda, K., H. Arakawa, T. Tanaka, K. Matsuda, C. Tanikawa, T. Mori, H. Nishimori, K. Tamai, T. Tokino, Y. Nakamura, and Y. Taya. 2000. p53AIP1, a potential mediator of p53-dependent apoptosis, and its regulation by Ser-46-phosphorylated p53. *Cell.* 102:849–862. http://dx.doi.org/10.1016/S0092-8674(00)00073-8

Okada, Y., M. Osada, S. Kurata, S. Sato, K. Aisaki, Y. Kageyama, K. Kihara, Y. Ikawa, and I. Katoh. 2002. p53 gene family p51(p63)-encoded, secondary transactivator p51B(TAp63alpha) occurs without forming an immunoprecipitable complex with MDM2, but responds to genotoxic

stress by accumulation. *Exp. Cell Res.* 276:194–200. http://dx.doi.org/10.1006/excr.2002.5535

Osada, M., M. Ohba, C. Kawahara, C. Ishioka, R. Kanamaru, I. Katoh, Y. Ikawa, Y. Nimura, A. Nakagawara, M. Obinata, and S. Ikawa. 1998. Cloning and functional analysis of human p51, which structurally and functionally resembles p53. *Nat. Med.* 4:839–843. http://dx.doi.org/10.1038/nm0798-839

Perez-Losada, J., D. Wu, R. DelRosario, A. Balmain, and J.H. Mao. 2005. p63 and p73 do not contribute to p53-mediated lymphoma suppressor activity in vivo. *Oncogene.* 24:5521–5524. http://dx.doi.org/10.1038/sj.onc.1208799

Petitjean, A., C. Cavard, H. Shi, V. Tribollet, P. Hainaut, and C. Caron de Fromentel. 2005. The expression of TA and DeltaNp63 are regulated by different mechanisms in liver cells. *Oncogene.* 24:512–519. http://dx.doi.org/10.1038/sj.onc.1208215

Polsky, D., K. Melzer, C. Hazan, K.S. Panageas, K. Busam, M. Drobnjak, H. Kamino, J.G. Spira, A.W. Kopf, A. Houghton, et al. 2002. HDM2 protein overexpression and prognosis in primary malignant melanoma. *J. Natl. Cancer Inst.* 94:1803–1806. http://dx.doi.org/10.1093/jnci/94.23.1803

Prince, S., S. Carreira, K.W. Vance, A. Abrahams, and C.R. Goding. 2004. Tbx2 directly represses the expression of the p21(WAF1) cyclin-dependent kinase inhibitor. *Cancer Res.* 64:1669–1674. http://dx.doi.org/10.1158/0008-5472.CAN-03-3286

Reis-Filho, J.S., P.T. Simpson, L.G. Fulford, A. Martins, and F.C. Schmitt. 2003a. P63-driven nuclear accumulation of beta-catenin is not a frequent event in human neoplasms. *Pathol. Res. Pract.* 199:785–793. http://dx.doi.org/10.1078/0344-0338-00497

Reis-Filho, J.S., P.T. Simpson, A. Martins, A. Preto, F. Gärtner, and F.C. Schmitt. 2003b. Distribution of p63, cytokeratins 5/6 and cytokeratin 14 in 51 normal and 400 neoplastic human tissue samples using TARP-4 multi-tumor tissue microarray. *Virchows Arch.* 443:122–132. http://dx.doi.org/10.1007/s00428-003-0859-2

Ribeiro-Silva, A., L.N. Zambelli Ramalho, S. Britto Garcia, and S. Zucoloto. 2003. The relationship between p63 and p53 expression in normal and neoplastic breast tissue. *Arch. Pathol. Lab. Med.* 127:336–340.

Riley, T., E. Sontag, P. Chen, and A. Levine. 2008. Transcriptional control of human p53-regulated genes. *Nat. Rev. Mol. Cell Biol.* 9:402–412. http://dx.doi.org/10.1038/nrm2395

Rocca, A., G. Viale, R.D. Gelber, L. Bottiglieri, S. Gelber, G. Pruneri, R. Ghisini, A. Balduzzi, E. Pietri, C. D'Alessandro, et al. 2008. Pathologic complete remission rate after cisplatin-based primary chemotherapy in breast cancer: correlation with p63 expression. *Cancer Chemother. Pharmacol.* 61:965–971. http://dx.doi.org/10.1007/s00280-007-0551-3

Rocco, J.W., C.O. Leong, N. Kuperwasser, M.P. DeYoung, and L.W. Ellisen. 2006. p63 mediates survival in squamous cell carcinoma by suppression of p73-dependent apoptosis. *Cancer Cell.* 9:45–56. http://dx.doi.org/10.1016/j.ccr.2005.12.013

Sakiz, D., T.T. Turkmenoglu, and F. Kabukcuoglu. 2009. The expression of p63 and p53 in keratoacanthoma and intraepidermal and invasive neoplasms of the skin. *Pathol. Res. Pract.* 205:589–594. http://dx.doi.org/10.1016/j.prp.2009.01.010

Sansome, C., A. Zaika, N.D. Marchenko, and U.M. Moll. 2001. Hypoxia death stimulus induces translocation of p53 protein to mitochondria. Detection by immunofluorescence on whole cells. *FEBS Lett.* 488:110–115. http://dx.doi.org/10.1016/S0014-5793(00)02368-1

Sato, T., F. Han, and A. Yamamoto. 2008. The biology and management of uveal melanoma. *Curr. Oncol. Rep.* 10:431–438. http://dx.doi.org/10.1007/s11912-008-0066-z

Satyamoorthy, K., N.H. Chehab, M.J. Waterman, M.C. Lien, W.S. El-Deiry, M. Herlyn, and T.D. Halazonetis. 2000. Aberrant regulation and function of wild-type p53 in radioresistant melanoma cells. *Cell Growth Differ.* 11:467–474.

Scatolini, M., M.M. Grand, E. Grosso, T. Venesio, A. Pisacane, A. Balsamo, R. Sirovich, M. Risio, and G. Chiorino. 2010. Altered molecular pathways in melanocytic lesions. *Int. J. Cancer.* 126:1869–1881.

Schilling, T., A. Kairat, G. Melino, P.H. Krammer, W. Stremmel, M. Oren, and M. Müller. 2010. Interference with the p53 family network contributes to the gain of oncogenic function of mutant p53 in hepatocellular carcinoma. *Biochem. Biophys. Res. Commun.* 394:817–823. http://dx.doi.org/10.1016/j.bbrc.2010.03.082

Seitz, S.J., E.S. Schleithoff, A. Koch, A. Schuster, A. Teufel, F. Staib, W. Stremmel, G. Melino, P.H. Krammer, T. Schilling, and M. Müller. 2010. Chemotherapy-induced apoptosis in hepatocellular carcinoma involves the p53 family and is mediated via the extrinsic and the intrinsic pathway. *Int. J. Cancer.* 126:2049–2066.

Senoo, M., J.P. Manis, F.W. Alt, and F. McKeon. 2004. p63 and p73 are not required for the development and p53-dependent apoptosis of T cells. *Cancer Cell.* 6:85–89. http://dx.doi.org/10.1016/j.ccr.2004.06.005

Senoo, M., F. Pinto, C.P. Crum, and F. McKeon. 2007. p63 Is essential for the proliferative potential of stem cells in stratified epithelia. *Cell.* 129:523–536. http://dx.doi.org/10.1016/j.cell.2007.02.045

Serber, Z., H.C. Lai, A. Yang, H.D. Ou, M.S. Sigal, A.E. Kelly, B.D. Darimont, P.H. Duijf, H. Van Bokhoven, F. McKeon, and V. Dötsch. 2002. A C-terminal inhibitory domain controls the activity of p63 by an intramolecular mechanism. *Mol. Cell. Biol.* 22:8601–8611. http://dx.doi.org/10.1128/MCB.22.24.8601-8611.2002

Shieh, S.Y., J. Ahn, K. Tamai, Y. Taya, and C. Prives. 2000. The human homologs of checkpoint kinases Chk1 and Cds1 (Chk2) phosphorylate p53 at multiple DNA damage-inducible sites. *Genes Dev.* 14:289–300.

Shields, J.A., C.L. Shields, M. Materin, T. Sato, and A. Ganguly. 2008. Role of cytogenetics in management of uveal melanoma. *Arch. Ophthalmol.* 126:416–419. http://dx.doi.org/10.1001/archopht.126.3.416

Smalley, K.S., R. Contractor, N.K. Haass, A.N. Kulp, G.E. Atilla-Gokcumen, D.S. Williams, H. Bregman, K.T. Flaherty, M.S. Soengas, E. Meggers, and M. Herlyn. 2007. An organometallic protein kinase inhibitor pharmacologically activates p53 and induces apoptosis in human melanoma cells. *Cancer Res.* 67:209–217. http://dx.doi.org/10.1158/0008-5472.CAN-06-1538

Sparrow, L.E., R. Soong, H.J. Dawkins, B.J. Iacopetta, and P.J. Heenan. 1995. p53 gene mutation and expression in naevi and melanomas. *Melanoma Res.* 5:93–100. http://dx.doi.org/10.1097/00008390-199504000-00004

Stretch, J.R., K.C. Gatter, E. Ralfkiaer, D.P. Lane, and A.L. Harris. 1991. Expression of mutant p53 in melanoma. *Cancer Res.* 51:5976–5979.

Suh, E.K., A. Yang, A. Kettenbach, C. Bamberger, A.H. Michaelis, Z. Zhu, J.A. Elvin, R.T. Bronson, C.P. Crum, and F. McKeon. 2006. p63 protects the female germ line during meiotic arrest. *Nature.* 444:624–628. http://dx.doi.org/10.1038/nature05337

Tokuyasu, K.T. 1980. Immunochemistry on ultrathin frozen sections. *Histochem. J.* 12:381–403. http://dx.doi.org/10.1007/BF01011956

Tuve, S., T. Racek, A. Niemetz, J. Schultz, M.S. Soengas, and B.M. Pützer. 2006. Adenovirus-mediated TA-p73beta gene transfer increases chemosensitivity of human malignant melanomas. *Apoptosis.* 11:235–243. http://dx.doi.org/10.1007/s10495-006-3407-0

Vance, K.W., S. Carreira, G. Brosch, and C.R. Goding. 2005. Tbx2 is overexpressed and plays an important role in maintaining proliferation and suppression of senescence in melanomas. *Cancer Res.* 65:2260–2268. http://dx.doi.org/10.1158/0008-5472.CAN-04-3045

Verhaegen, M., A. Checinska, M.B. Riblett, S. Wang, and M.S. Soengas. 2012. E2F1-dependent oncogenic addiction of melanoma cells to MDM2. *Oncogene.* 31:828–841. http://dx.doi.org/10.1038/onc.2011.277

Walerych, D., G. Kudla, M. Gutkowska, B. Wawrzynow, L. Muller, F.W. King, A. Helwak, J. Boros, A. Zylicz, and M. Zylicz. 2004. Hsp90 chaperones wild-type p53 tumor suppressor protein. *J. Biol. Chem.* 279:48836–48845. http://dx.doi.org/10.1074/jbc.M407601200

Walerych, D., M.B. Olszewski, M. Gutkowska, A. Helwak, M. Zylicz, and A. Zylicz. 2009. Hsp70 molecular chaperones are required to support p53 tumor suppressor activity under stress conditions. *Oncogene.* 28:4284–4294. http://dx.doi.org/10.1038/onc.2009.281

Wäster, P.K., and K.M. Ollinger. 2009. Redox-dependent translocation of p53 to mitochondria or nucleus in human melanocytes after UVA- and UVB-induced apoptosis. *J. Invest. Dermatol.* 129:1769–1781. http://dx.doi.org/10.1038/jid.2008.421

Weiss, J., M. Heine, K.C. Arden, B. Körner, H. Pilch, R.A. Herbst, and E.G. Jung. 1995. Mutation and expression of TP53 in malignant melanomas. *Recent Results Cancer Res.* 139:137–154. http://dx.doi.org/10.1007/978-3-642-78771-3_10

Westfall, M.D., A.S. Joyner, C.E. Barbieri, M. Livingstone, and J.A. Pietenpol. 2005. Ultraviolet radiation induces phosphorylation and ubiquitin-mediated degradation of DeltaNp63alpha. *Cell Cycle*. 4: 710–716. http://dx.doi.org/10.4161/cc.4.5.1685

Whitesell, L., and S.L. Lindquist. 2005. HSP90 and the chaperoning of cancer. *Nat. Rev. Cancer.* 5:761–772. http://dx.doi.org/10.1038/nrc1716

Yamamoto, K., H. Ichijo, and S.J. Korsmeyer. 1999. BCL-2 is phosphorylated and inactivated by an ASK1/Jun N-terminal protein kinase pathway normally activated at G(2)/M. *Mol. Cell. Biol.* 19:8469–8478.

Yamamoto, M., H. Takahashi, K. Saitoh, T. Horikoshi, and M. Takahashi. 1995. Expression of the p53 protein in malignant melanomas as a prognostic indicator. *Arch. Dermatol. Res*. 287:146–151. http://dx.doi.org/10.1007/BF01262323

Yang, A., and F. McKeon. 2000. P63 and P73: P53 mimics, menaces and more. *Nat. Rev. Mol. Cell Biol.* 1:199–207. http://dx.doi.org/10.1038/35043127

Yang, A., M. Kaghad, Y. Wang, E. Gillett, M.D. Fleming, V. Dötsch, N.C. Andrews, D. Caput, and F. McKeon. 1998. p63, a p53 homolog at 3q27-29, encodes multiple products with transactivating, death-inducing, and dominant-negative activities. *Mol. Cell.* 2:305–316. http://dx.doi.org/10.1016/S1097-2765(00)80275-0

Yaziji, H., and A.M. Gown. 2003. Immunohistochemical markers of melanocytic tumors. *Int. J. Surg. Pathol*. 11:11–15. http://dx.doi.org/10.1177/106689690301100103

Zangen, R., E. Ratovitski, and D. Sidransky. 2005. DeltaNp63alpha levels correlate with clinical tumor response to cisplatin. *Cell Cycle*. 4: 1313–1315. http://dx.doi.org/10.4161/cc.4.10.2066

Zerp, S.F., A. van Elsas, L.T. Peltenburg, and P.I. Schrier. 1999. p53 mutations in human cutaneous melanoma correlate with sun exposure but are not always involved in melanomagenesis. *Br. J. Cancer.* 79:921–926. http://dx.doi.org/10.1038/sj.bjc.6690147